

Title:

Small RNA-mediated genomic silencing promotes
telomere stability in the absence of telomerase

Authors:

Charlie Longtine^{1,2,#}, Stephen Frenk^{1,2,#}, and Shawn Ahmed^{1,2*}

Affiliations:

¹Department of Genetics, ²Department of Biology, University of North Carolina, Chapel
Hill, NC, USA

Equal contributions

*Correspondence and Lead Contact: shawn@med.unc.edu

Short title: small RNAs promote telomere stability

Abstract

Telomerase deficiency in human somatic cells results in telomere erosion and senescence. Small RNAs that target telomeres have been observed in diverse organisms but their functions are not well characterized. We define an endogenous small RNA pathway in *Caenorhabditis elegans* that promotes heterochromatin formation at telomeres via Dicer, the perinuclear Argonaute protein WAGO-1 and the nuclear Argonaute protein HRDE-1. Loss of telomerase induces biogenesis of siRNAs that target the telomeric lncRNA TERRA, whereas loss of both telomerase and small RNA-mediated telomeric silencing induces TERRA expression, DNA damage, and an accelerated sterility phenotype. These phenotypes can be rescued by exogenous telomeric siRNAs or by loss of the DNA damage response protein EXO-1. Thus, endogenous siRNAs interact with TERRA to promote heterochromatin formation in a manner that is critical for the stability of naturally eroding telomeres. We propose that small RNA-mediated genome silencing could be broadly relevant to regulation of proliferative aging.

Introduction

Telomeres are repetitive nucleoprotein structures that protect the ends of linear eukaryotic chromosomes from degradation and recognition as double-stranded DNA breaks (Maciejowski and de Lange, 2017, Shay, 2016). In most human somatic cells, which are deficient for telomerase reverse transcriptase, telomeres erode over progressive cell divisions, eventually triggering replicative senescence (Holohan et al., 2014, Shay, 2016). Telomere shortening thus acts as a barrier to tumorigenesis, but may also contribute to organismal aging through impaired stem cell function, regeneration, and organ maintenance (Donate and Blasco, 2011, Shay, 2016). Regulating the rate of telomere erosion in telomerase-negative cells is therefore crucial to maintain this balance between tumor suppression and age-related tissue decline (Li et al., 2017, Maciejowski and de Lange, 2017). Tumor cells escape telomere-triggered senescence by stabilizing telomere length, either through reactivation of telomerase or through activation of the telomerase-independent recombination-mediated telomere

maintenance pathway termed Alternative Lengthening of Telomeres (ALT) (Pickett and Reddel, 2015).

Telomeres have features characteristic of heterochromatin in that they associate with the heterochromatin protein HP1 and contain transcriptionally repressive histone marks such as methylation of H3K9 and H4K20 (Benetti et al., 2007, McMurchy et al., 2017). Nonetheless, telomeres are transcribed into the G-rich long noncoding RNA (lncRNA) termed TERRA, a feature widely conserved among eukaryotes, and lower levels of the C-rich antisense lncRNA ARRET have also been reported (Azzalin et al., 2007). TERRA is transcribed from the subtelomere into the telomere by RNA polymerase II and is upregulated at shortened and damaged telomeres, where it may recruit telomerase and chromatin modifiers to promote telomere elongation (Azzalin and Lingner, 2015, Cusanelli et al., 2013). Telomere elongation represses expression of TERRA through increased methylation and HP1 binding (Arnoult et al., 2012). Notably, telomere shortening in mice with telomerase defects and overexpression of a negative regulator of telomere length have been associated with loss of heterochromatic marks at telomeres and subtelomeres (Benetti et al., 2007, Benetti et al., 2008).

Transcriptional silencing and heterochromatin deposition at repetitive segments of the genome such as the pericentromere (Holoch and Moazed, 2015, Reinhart and Bartel, 2002) require long non-coding RNA (lncRNA) transcripts that promote biogenesis of and interact with small RNAs that direct heterochromatin factors to target genomic loci. Endogenous sources of double-stranded RNA such as sense-antisense transcript hybrids can be processed into small RNAs that play roles in creating and maintaining siRNA-mediated heterochromatin, where paradoxically RNA expression is required for genomic silencing. Bidirectional transcription of telomeres has been linked to production of telomeric siRNAs that promote subtelomeric DNA methylation in *Arabidopsis* (Vrbsky et al., 2010). The presence of similar telomeric siRNAs has also been observed in *Tetrahymena*, mouse stem cells, and human cell lines (Cao et al., 2009, Rossiello et al., 2017), but their functional relevance at canonical telomeres is not well understood in any experimental system.

Germline transcription in *C. elegans* is regulated in part by a network of small RNA pathways that promote silencing or expression of target loci in a sequence-specific manner (Billi et al., 2014). Transcription of potentially harmful foreign genetic elements including transposons and transgenes is repressed by 21 nucleotide PIWI-interacting RNAs or piRNAs. These interact with PRG-1, a member of the PIWI clade of Argonaute proteins that recognizes RNA targets of piRNAs based on sequence complementarity with up to 3 mismatches (Bagijn et al., 2012, Batista et al., 2008, Das et al., 2008). RNA target recognition triggers the recruitment of RNA-dependent RNA polymerases (RdRPs) that act in Mutator bodies, which are associated with perinuclear P granules, to create *de novo* 22 nucleotide secondary siRNAs with a 5' guanine (22G RNAs) (Pak and Fire, 2007). These 22G RNAs are loaded onto worm-specific Argonaute proteins (WAGOs) such as the nuclear WAGO HRDE-1, which promotes heterochromatin deposition at target loci (Ashe et al., 2012, Buckley et al., 2012). Germline transcription is protected by a separate set of 22G RNAs that interact with the anti-silencing Argonaute protein CSR-1 (Avgousti et al., 2012, Wedeles et al., 2013). Aside from the piRNA pathway, 22G activity can be triggered by primary siRNAs from other sources. For example, DCR-1, the *C. elegans* homologue of the highly conserved RNase class III enzyme Dicer, can cleave endogenous and exogenous double stranded RNA transcripts to create primary 26G RNAs, which bind a distinct set of Argonautes to trigger target silencing through the 22G pathway described above (Bernstein et al., 2001, Ketting et al., 2001, Knight and Bass, 2001).

Here we describe an endogenous siRNA pathway that represses TERRA via heterochromatin formation and functions redundantly with telomerase to promote telomere stability.

Results

Loss of endogenous siRNAs or XNP-1/ATRX does not promote ALT

High levels of TERRA and loss of the histone H3.3 chaperone subunits ATRX and DAXX commonly occur in human ALT cancers (Flynn et al., 2015, Lovejoy et al., 2012). The ATRX/DAXX complex mediates histone H3.3 incorporation at telomeres and interacts with methylated H3K9 and HP1 to promote heterochromatin formation (Wong et al., 2010), which has been proposed to repress ALT by protecting telomeres from replication stress and TERRA expression (Udugama et al., 2015). We have previously shown that 10-20% of *C. elegans* strains that are deficient for telomerase can be maintained indefinitely through the activation of ALT (Cheng et al., 2012). Because human ALT cancers are characterized by ATRX-mediated heterochromatin dysfunction, we reasoned that small RNA factors that promote heterochromatin silencing might regulate the establishment of ALT. We tested this hypothesis by passaging *trt-1* telomerase mutant strains that were deficient for biogenesis of either primary or secondary siRNAs by transferring 100s of worms per strain weekly, which reliably allows survival of 10-20% of strains via ALT (Cheng et al., 2012). Loss of either primary siRNAs (*trt-1; dcr-1*) or downstream secondary siRNAs (*trt-1; mut-7* and *trt-1; mut-14*) did not significantly alter the proportion of strains that survive via ALT (Figure 1A, Table S1). Similarly, loss of the histone H3.3 chaperone XNP-1/ATRX itself did not affect the establishment or maintenance of ALT (Table S1), indicating that loss of neither siRNA- nor XNP-1/ATRX-mediated heterochromatin formation is sufficient to promote ALT.

Small RNA and heterochromatin factors repress rapid sterility when telomerase is deficient

C. elegans strains mutant for telomerase reverse transcriptase, *trt-1*, become uniformly progressively sterile – analogous to crisis that is induced by telomere erosion, chromosome fusion and genome catastrophe in checkpoint-deficient telomerase-negative mammalian cells – when 6 worms are passaged weekly (Ahmed and Hodgkin, 2000), which eliminates survival via ALT (Cheng et al., 2012). Intriguingly, when passaged by transferring 6 L1 larvae per week, *trt-1* mutant lines lacking primary or secondary siRNA biogenesis factors became sterile significantly faster than *trt-1* single mutants (Figure 1B, Table S2). siRNA-deficient *trt-1* strains rapidly accumulated end-to-end chromosome fusions by generation F12, a characteristic of telomerase mutants

that have grown for more than 20 generations (Figure 1G). These strains also displayed high levels of DNA damage by generation F6 that were not observed for *trt-1* single mutant controls (Figure 1H). As oocyte karyotypes can only reliably detect the presence of multiple chromosome fusions, we performed genetic crosses that would be capable of detecting a single heterozygous end-to-end chromosome fusion (Ahmed and Hodgkin, 2000). Chromosome fusions cause non-disjunction events during meiosis that elicit dominant embryonic lethality or XO male phenotypes in progeny of heterozygous F1 animals. We crossed four independent *trt-1 dcr-1* F4 hermaphrodites and failed to detect fused chromosomes that were present in generation F24 *trt-1* mutant controls ($p = 3.841e-05$ for males and $p = 3.61e-05$ for dead embryos, Mann Whitney U test) (Table S3). Together, these results suggest that loss of small RNAs and telomerase elicits telomere damage but not telomere fusions in early generations, and that the rapid sterility of these strains in later generations is promoted by critically shortened telomeres that give rise to abundant end-to-end chromosome fusions. Small RNA factors required to prevent this accelerated sterility included RDE-4, which binds endogenous dsRNA and forms a complex with the Dicer nuclease DCR-1, and the Argonaute RDE-1, which acts with the RNA-dependent RNA polymerase RRF-3 to promote production of dsRNA-derived primary siRNAs (Gent et al., 2010, Steiner et al., 2009, Tabara et al., 2002) (Figure 1B). The MUTATOR proteins MUT-7 and MUT-14, which also were required to prevent rapid sterility in *trt-1* (Figure 1B), promote amplification of 22G secondary siRNAs that act as downstream effector siRNAs by promoting mRNA degradation in the cytoplasm or transcriptional silencing in the nucleus (Billi et al., 2014, Ketting et al., 1999, Tijsterman et al., 2002).

Southern blotting suggested that *dcr-1* and *mut-14* single mutants do not have shorter telomeres than wildtype or *trt-1* mutant strains (Figure S1), which implies that the accelerated sterility of small RNA-deficient *trt-1* mutant strains is unlikely to be a consequence of short telomeres that are inherited from gametes of small RNA-deficient grandparents. We tested this premise using genetics, by crossing a *trt-1; dcr-1* double mutant hermaphrodite with *dcr-1* mutant males, singling *trt-1 +/-; dcr-1 -/-* F1 hermaphrodites and isolating *trt-1; dcr-1* double mutant F2. This cross was repeated 15

times, to create a *trt-1*; *dcr-1* double mutant strain whose telomeres should be exclusively derived from the *dcr-1* mutant background. The *trt-1*; *dcr-1* 15x strain became sterile slightly more slowly than freshly created *trt-1*; *dcr-1* double mutants ($p = 0.07$) (Fig. 1H), indicating that shortened telomeres transmitted from the *dcr-1* mutant cannot explain the rapid sterility of *trt-1*; *dcr-1* double mutants. Because none of the small RNA single mutants tested became progressively sterile or accumulated chromosome fusions (Figure 1G), we conclude that telomere maintenance is not impaired in small RNA-deficient lines in the presence of telomerase. We analyzed the dynamics of telomere erosion using terminal restriction fragment analysis, but did not observe an obvious difference between *trt-1* and siRNA-deficient *trt-1* mutant strains (Figure S2). Two other small RNA factors, RRF-2 and ERI-1, were not required to prevent rapid onset of sterility, indicating that the endogenous siRNA pathway that requires ERI-1 (Gent et al., 2010, Han et al., 2009) is dispensable for telomere protection in the absence of telomerase (Figure 1B).

We hypothesized that small RNAs might repress rapid sterility by directing chromatin factors to telomeres to promote deposition of heterochromatic marks. *C. elegans* telomeres have previously been reported to be enriched for H3K9me2 and bound by the HP1 homolog HPL-2, which promotes H3K9me2 deposition and heterochromatin formation, but not by the other *C. elegans* HP1 homolog HPL-1, which interacts with H3K9me3 (Canzio et al., 2014, McMurphy et al., 2017). We confirmed that H3K9me2 but not H3K9me3 was enriched at *C. elegans* telomeres using high throughput sequencing data sets generated from chromatin immunoprecipitation (ChIP) experiments performed by independent groups (McMurphy et al., 2017, Zeller et al., 2016). Moreover, we observed small H3K9me2 domains that extended into the subtelomere at all twelve *C. elegans* chromosome ends (Figure 3A-D). H3K4 methylation, which is associated with regions of active transcription, must be removed by demethylases prior to deposition of repressive H3K9 methylation (Greer et al., 2010, Li et al., 2008). Similar to primary and secondary siRNA-deficient *trt-1* strains, loss of HPL-2 but not HPL-1, and loss of either of the two *C. elegans* H3K4 demethylases RBR-2/KDM5 or SPR-5/LSD1, caused accelerated senescence in *trt-1* mutants (Figure

1C). Thus, H3K4 demethylation and H3K9me2 deposition prevent telomere instability in the absence of telomerase.

The histone remodeling protein XNP-1/ATRX has previously been implicated in telomeric heterochromatin formation and interacts with unmethylated H3K4 and methylated H3K9 deposited on the histone variant H3.3 (Udugama et al., 2015). *trt-1 xnp-1* double mutants went sterile significantly faster than *trt-1* single mutants but not as fast as small RNA deficient *trt-1; mut-7* double mutants (Figure 1D). This suggests that XNP-1 may mediate some, but not all heterochromatin formation at telomeres, possibly because siRNA-dependent methylation of histones other than H3.3, such as canonical histone H3 or H4 can promote telomere stability. Additionally, because loss of both XNP-1 and MUT-7 did not cause an additive effect on survival in *trt-1* mutant strains (Figure 1D), these genes may function in the same pathway, which implies that siRNAs direct the chromatin remodeler XNP-1 to telomeres to repress rapid sterility in the absence of telomerase.

Increased expression of TERRA in small RNA and chromatin deficient *trt-1* strains

We hypothesized that DCR-1 and RDE-4 may interact with telomeric dsRNA produced from bidirectional transcription of telomeres into TERRA and ARRET, to create primary siRNAs that are then amplified into a secondary siRNA population that triggers small RNA-dependent silencing of TERRA (Rossiello et al., 2017, Vrbsky et al., 2010). To test whether small RNA and chromatin factors regulate telomeric transcription we measured the abundance of TERRA by qRT-PCR at three chromosome ends using primers within their H3K9me2-coated subtelomere domains (Figure 3A-D). Compared to *trt-1* single mutant controls, TERRA was upregulated in early-generation *trt-1; rde-4*, and *trt-1; mut-14* and *trt-1; spr-5* double mutants (Figure 2A). These high levels of TERRA transcription were markedly induced in small RNA and heterochromatin mutants that lacked telomerase, consistent with the hypothesis that TERRA transcription is specifically induced at damaged or shortened telomeres (Porro et al., 2014, Rossiello et al., 2017).

We next used RNA Fluorescence *In Situ* Hybridization (FISH) to confirm the effects on TERRA expression and to examine its cell and tissue localization. In wildtype control and *trt-1* mutant hermaphrodite and male worms, TERRA was expressed at low levels in the soma as well as the pachytene region of the meiotic germline (Figures 2B-D, S3-4), which corresponds to the location of several lncRNA-mediated germline silencing processes (Taylor et al., 2015), including Meiotic Silencing of Sex Chromosomes in mammals and *C. elegans* (Heard and Turner, 2011) and a transcriptional burst of piRNAs in mammals that primes genomic silencing in germ cells prior to gametogenesis (Gou et al., 2014). Compared to both wildtype control and *trt-1* or *dcr-1* single mutant strains, *trt-1; dcr-1* double mutant strains had increased expression of TERRA in the germline (Figures 2B-D, S3) and soma (Figures S3-4) by the F6 generation. Endogenous siRNAs thus regulate telomeric transcription in both the soma and germline during telomere attrition, likely through the production of siRNAs that directly target the heterochromatin factors HPL-2, RBR-2 and SPR-5 to telomeres.

Subtelomeric siRNAs are upregulated in telomerase mutants

Telomeric siRNAs have been observed in protists, plants and mammals (Cao et al., 2009, Vrbisky et al., 2010). We therefore interrogated 92 publicly available small RNA sequencing libraries created from RNA isolated from various *C. elegans* strains and found rare reads that mapped perfectly to the *C. elegans* telomere repeat (TTAGGC)_n, occurring at a frequency of 1 per 10,000,000 reads. piRNAs with up to 3 mismatches can target regions of the *C. elegans* genome for silencing (Bagijn et al., 2012), and we found that telomeric siRNAs with up to 3 mismatches were substantially more abundant than those with perfect telomere repeat sequence (1 per 100,000). Telomeric siRNAs with zero to two mismatches were significantly more likely to be composed of the telomeric G-strand sequence than would be expected by chance ($p < 2.2e-16$, binomial test) (Figure 3E). The proportion of telomeric siRNAs with one or two mismatches beginning with a G nucleotide was significantly greater than that for all mappable reads ($p < 1e-15$, Fisher's exact test) and the median length for these RNAs was 22 nucleotides (Figure 3D, F), suggesting that telomeric siRNAs mapping imperfectly to telomeres are enriched for 22G RNA species. This is consistent with the model that

primary siRNAs recruit RNA-dependent RNA polymerases to target RNAs in order to create secondary effector siRNA populations de novo that are highly enriched for 22G RNAs (Gu et al., 2009). We compared levels of telomeric siRNAs from wild-type with those of small RNA mutants that promote telomere stability in the absence of telomerase, such as *dcr-1*, *rde-4*, *mut-7*, *mut-14*, and found that levels of telomeric siRNAs were sometimes depleted in these backgrounds, but not always (File S1).

Given that telomeric siRNAs are rare in small RNA sequencing data sets, we hypothesized that loss of telomerase might elicit production of telomeric siRNAs in a manner that might depend on Dicer. We therefore isolated RNA from wildtype control, *trt-1* single mutant, and *trt-1; dcr-1* double mutant strains and prepared small RNA libraries. We sequenced these libraries deeply in an effort to detect rare telomeric siRNAs. We obtained ~20,000,000 reads each for 6 data sets and found that our *trt-1 dcr-1* data sets were strongly depleted of 22G RNAs that were previously reported to depend on *dcr-1* (Figure S5A) (Gent et al., 2010). To assess TRT-1-dependent changes in siRNAs throughout the genome, we counted the number of 22G reads mapping uniquely antisense to protein-coding genes and found upregulation of siRNAs at 720 loci and downregulation at 456 loci in *trt-1* animals compared with wild-type (Figure S5B). Of the upregulated loci, 465 were not upregulated in *trt-1; dcr-1* animals compared with wild-type, indicating DCR-1 dependence. We did not find significant GO terms in loci with either up or downregulated siRNA production. Given the importance of both TRT-1 and siRNAs in germline function, we asked whether the loci with differential siRNA production were enriched for germline-enriched genes. We used previously published data on germline expression (Ortiz et al., 2014) and found significant enrichment for germline-enriched genes in both upregulated and downregulated loci ($p < 1e-19$ and $p < 1e-33$ respectively, Pearson's Chi Square test with Bonferroni correction) (Figure S5C). This may reflect a form of epigenome dysregulation within germ cells that occurs as a consequence of telomerase deficiency. siRNAs mapping to transposons were unaffected by loss of TRT-1, with the exception of the CER-10 LTR retrotransposon, for which siRNAs were three-fold downregulated (Figure S5D).

We detected no siRNAs composed of perfect telomere repeats in any genetic background, but found some with up to 3 mismatches, whose levels did not change substantially in siRNAs from *trt-1* single mutants or *trt-1; dcr-1* double mutants (Figure 4A). We next examined 22G RNAs at subtelomeric regions (defined as the 2kb of sequence adjacent to the telomere) and found that these were present in wildtype samples at the left end of chromosome III, and that their abundance was increased two-fold in *trt-1* single mutants and their presence almost entirely eliminated in *trt-1; dcr-1* double mutants (Figure 4C, E). Subtelomeric siRNAs were also observed within 1kb of the telomere at the left ends of chromosomes I and IV in *trt-1* mutants and not in wildtype or *trt-1; dcr-1* double mutants (Figure 4B, D). The right ends of Chromosomes I and III and the left end of Chromosome II all showed at least a two-fold increase in subtelomeric siRNAs in *trt-1* and/or *trt-1; dcr-1* double mutants (Figure 4E). We observed a significant bias for subtelomeric siRNAs whose sequences correspond to the C-rich telomere strand (antisense to TERRA) for the left arms of Chromosomes I and III ($p < 1e-13$ and $p < 1e-43$ respectively, binomial test with Bonferroni correction) and for the right arm of Chromosome I ($p < 1e-172$, binomial test with Bonferroni correction) while the nucleotide sequences of subtelomeric siRNAs at the left arm of Chromosome IV and the right arm of Chromosome III showed a bias for subtelomeric TERRA, suggesting that they were created from ARRET ($p < 1e-11$, $p = 0.006$ respectively, binomial test with Bonferroni correction) (Figure 4F). These observations suggest that telomere dysfunction triggers the upregulation of small RNA biogenesis at multiple subtelomeres, through both DCR-1-dependent and -independent mechanisms.

We next studied data sets of small RNAs that immunoprecipitate with HRDE-1 and WAGO-1, Argonaute proteins that promote silencing in the germline, as well as with the germline anti-silencing Argonaute CSR-1 (Table S3). Enrichment of small RNAs for each protein was calculated by dividing the number of reads in the immunoprecipitate library by the number of reads in the corresponding input library. Telomeric siRNAs were enriched in WAGO-1 immunoprecipitates relative to input, but this was not the case for HRDE-1 or CSR-1 (Figure 3G). Enrichment of subtelomeric small RNAs in WAGO-1 was detected at all chromosome ends tested apart from the right arm of Chromosome I

(some chromosome ends were not tested due to an absence of reads in the input library). Enrichment was also detected for HRDE-1 at all chromosome ends excluding the right arm of Chromosome *I* and the left arm of Chromosome *III* (Figure 3H). Interestingly, CSR-1 showed the opposite pattern of enrichment to WAGO-1 and HRDE-1, with enrichment at none of the chromosome ends apart from the right end of Chromosome *I*. The ribosomal DNA, the most highly expressed locus in the *C. elegans* genome, is immediately adjacent to this telomere (Wicky et al., 1996), and it is therefore possible that siRNA activity takes a predominantly anti-silencing function at this chromosome end. We asked if either Argonaute that associates with telomeric or sub-telomeric siRNAs, WAGO-1 or to a lesser degree HRDE-1, promotes telomere maintenance in the absence of telomerase and found that both *wago-1 trt-1* and *trt-1; hrde-1* double mutants displayed rapid sterility phenotypes in comparison to *trt-1* single mutants ($p < 1e-11$ and $p < 1e-12$, respectively, log rank test) (Figure 1E).

Telomeric siRNAs and loss of EXO-1 repress sterility in the absence of telomerase

Although we failed to detect siRNAs with perfect telomere repeat sequence in our siRNA data sets, these were present at very low levels in data sets generated by other groups (Figure 3D-F) and could be difficult to detect for technical reasons. We hypothesized that if loss of small RNAs directly targeting the telomere were responsible for the rapid sterility in siRNA-deficient *trt-1*, then reintroduction of exogenous telomeric siRNAs might rescue this phenotype. To address this experimentally, we used a viable *dcr-1* allele, *mg375*, which is deficient for endogenous siRNA production but is hypersensitive to exogenous RNAi when fed *E. coli* expressing dsRNA (Welker et al., 2010). *trt-1; dcr-1(mg375)* double mutants that were passaged on bacteria expressing telomeric dsRNA remained fertile significantly longer than those expressing dsRNA from an empty vector control (Figure 4A). This delay of sterility did not occur for *trt-1* single mutant controls. Moreover, *trt-1; dcr-1(mg375)* strains fed telomeric dsRNA had markedly reduced levels of DNA damage at F6 in comparison to *trt-1; dcr-1(mg375)* strains grown on control RNAi or on regular OP50 bacteria that do not express dsRNA (Figure 1F, 5C).

In budding yeast, artificially-induced TERRA overexpression promotes telomere shortening *in cis* by forming RNA:DNA hybrids that stall telomeric replication forks as well as by stimulating telomeric resection by Exo1 (Maicher et al., 2012, Pfeiffer and Lingner, 2012). We therefore hypothesized that loss of EXO-1 might rescue the accelerated sterility phenotype in siRNA-deficient telomerase mutants. *trt-1; exo-1; mut-14* triple mutant lines survived significantly longer than *trt-1; mut-14* double mutants (Figure 5B) and showed reduced DNA damage and expression of moderate levels of TERRA at F6 (Figures 5B, S5). Moreover, *trt-1; exo-1* double mutant controls remained fertile even longer than *trt-1* single mutants (Figure 5B), indicating that EXO-1-mediated resection promotes telomere-shortening-induced senescence in the absence of telomerase, both at normal telomeres and at telomeres lacking siRNA-mediated silencing. While *trt-1; exo-1* double mutant controls remained fertile longer than *trt-1* single mutants, this was not true for *trt-1* single mutants grown on exogenous telomeric dsRNA (Figure 5A, B). Thus, although loss of *exo-1* rescues the rapid sterility phenotype in small RNA-deficient telomerase mutants, resection by EXO-1 also likely promotes telomere shortening in *trt-1* single mutants independent of siRNA production and telomeric heterochromatin structure.

Discussion

We propose the following model, based in part on our observations: upon telomere shortening or damage, TERRA expression is transiently induced, which may recruit telomerase (Moravec et al., 2016). If telomerase is present, shortened telomeres are elongated. When telomerase is deficient, TERRA expression is suppressed via an endogenous small RNA pathway that interacts with TERRA to facilitate telomeric heterochromatin deposition. We observed upregulation of telomeric and subtelomeric siRNAs in telomerase mutants, which may act as a negative feedback mechanism to maintain appropriate levels of TERRA in the absence of telomerase. H3K9me2 but not H3K9me3 is present at wildtype *C. elegans* telomeres, and we found that the *C.*

C. elegans HP1 homolog HPL-2 that binds to and specifically stabilizes H3K9me2 (McMurchy et al., 2017) represses telomere instability in the absence of telomerase. We therefore propose that siRNAs function at naturally eroding telomeres to promote heterochromatin formation in a manner that suppresses a form of replication-dependent DNA damage that activates transcription of TERRA and associated small RNAs. However, when small RNAs fail to promote heterochromatin formation at telomeres in the absence of telomerase, our data suggest that EXO-1-mediated DNA damage then leads to dysfunctional telomeres accompanied by high levels of TERRA that are observed in early-generation *trt-1; dcr-1* double mutants (Figure 5). Importantly, loss of EXO1 in telomerase-negative mice has been shown to extend lifespan and improve organ maintenance by repressing ssDNA formation and the DNA damage response (Schaetzlein et al., 2007), suggesting a conserved role for Exonuclease-1 in the metazoan response to dysfunctional telomeres. It is possible that heterochromatin creates a more compact telomere architecture that is resistant to nucleolytic attack by EXO-1. Alternatively, damage signaling from eroding telomeres may recruit EXO-1 and other DNA damage factors.

Our results demonstrating that high levels of TERRA are associated with telomere instability might be consistent with a role for TERRA expression in the DNA damage response as discussed by two recent studies. First, in mammals TERRA expression occurs in response to a distinct form of telomeric damage - acutely deprotected, non-replicating telomeres in the presence of telomerase – and is accompanied by production of telomeric siRNAs that promote DNA damage response factor recruitment (Rossiello et al., 2017). Second, a recent study in *S. cerevisiae* showed that increased TERRA expression and persistent telomeric R-loops in telomerase mutants can repress senescence by promoting recombination, indicating that increased levels of TERRA can in some contexts be beneficial (Graf et al., 2017). Our observations that high levels of TERRA are induced in telomerase negative small RNA mutants in response to EXO-1 (Figure 5), suggest that TERRA may be induced by or integral to a telomeric DNA damage response.

We detected subtelomeric siRNAs that were dependent on Dicer and that interacted with the Argonaute proteins WAGO-1 and HRDE-1 (Figure 3H), both of which promoted telomere stability in the absence of telomerase. These Argonaute proteins are known to be active in the germline and bind to RdRP-generated 22G RNAs that target overlapping groups of transcripts, including genes, transposons and pseudogenes (Gu et al., 2009). Moreover, WAGO-1 localizes to perinuclear P-granules (or germ granules), where it could promote either transcriptional or post-transcriptional gene silencing (Gu et al., 2009), whereas HRDE-1 is localized to the nucleus where it promotes transcriptional gene silencing. The *C. elegans* Piwi homolog PRG-1 also localizes to P granules, where it interacts with piRNAs to promote the biogenesis of secondary 22G RNAs that may interact with HRDE-1 molecules that transiently enter P granules before entering the nucleus to promote heterochromatin silencing. Moreover, HRDE-1 and WAGO-1 have been shown to function redundantly to promote transgenerational epigenomic silencing of transgenes, a form of permanent epigenomic silencing that is initiated by PRG-1/Piwi and associated piRNAs (Ashe et al., 2012, Buckley et al., 2012). Given that HRDE-1 and WAGO-1 interact with 22G siRNAs that map to distinct and overlapping subtelomeres, we propose that these Argonaute proteins collaborate to promote heterochromatin formation at subtelomeres, such that both P-granule localized WAGO-1 and nuclear Argonaute HRDE-1 play important roles in this silencing process. Although proteomics has been performed for both HRDE-1 and WAGO-1, these Argonaute proteins do not physically interact with one another or possess common interacting proteins (Akay et al., 2017, Shirayama et al., 2014). We propose that EXO-1-mediated telomere resection is accompanied by expression of TERRA and ARRET, resulting in low levels of dsRNA that would elicit Dicer recruitment via RDE-4 to create a primary siRNA population that would be amplified by RdRPs to create 22G RNAs that associate with WAGO-1 and HRDE-1 to promote telomeric silencing (Figure 6).

We did not detect any telomeric siRNAs lacking mismatches in our analysis of siRNAs from telomerase mutants, nor could we identify Dicer-dependent telomeric siRNAs that had mismatches. However, we did find that exogenous telomeric siRNAs were able to

complement the premature sterility of *trt-1 dcr-1* mutants (Figure 4A). Together, our results suggest that while telomeric siRNAs can promote telomere stability in the absence of telomerase, that subtelomeric transcripts are templates for *de novo* synthesis of endogenous siRNAs that are relevant to telomere repeat stability. Consistently, TERRA transcription in *S. pombe* initiates in the subtelomere but rarely extends into the telomere (Moravec et al., 2016). We propose that TERRA is not significantly expressed in RNAi deficient mutants that possess wildtype telomerase, because telomerase is capable of healing telomeric damage that occurs in the absence of small RNA-mediated heterochromatin formation.

Small RNAs promote genomic silencing of many types of transposons and are essential for the stability of *Drosophila melanogaster* telomeres, which are composed of non-LTR retrotransposons that are distinct from the simple repetitive sequences that are maintained by telomerase and cap chromosome ends in most organisms (Pardue and DeBaryshe, 2003). siRNAs function at *Drosophila* telomeres to promote heterochromatin-mediated genome silencing via the *Drosophila* homologs of HP1 and ATRX, thereby preventing telomere instability (Chavez et al., 2017, Fulcher et al., 2014). Small RNA-mediated control of telomere stability through regulation of heterochromatin is therefore a conserved feature of both non-canonical and canonical telomeres. siRNA dysfunction at *Drosophila* telomeres leads to immediate telomere deprotection and fusion in embryos, whereas *C. elegans* siRNA mutants telomeres have normal lengths (Figure S1). When both telomerase and *C. elegans* siRNA factors are removed, telomeres trigger a DNA damage response in many germ cells but this does not result in telomere fusions for several generations, each generation representing 8-10 cell divisions. This indicates that the accelerated sterility phenotype of siRNA-deficient *trt-1* mutants is not a consequence of a defect in acute telomere uncapping, but rather an acceleration of the onset of crisis. We speculate siRNA-mediated heterochromatin formation at telomeres modulates the stability of telomeres in diverse organisms that maintain their telomeres via telomerase-mediated telomere repeat addition.

Since most human somatic cells do not express telomerase, our findings may be generally relevant to understanding how cells control the rate of telomere shortening in the absence of telomerase through modulation of telomeric transcription and chromatin either in the germ cells, in the early embryo or in adult somatic cells. Increased TERRA expression and telomeric R-loops have been reported to associate with high levels of DNA damage in ICF syndrome cells, which are deficient for DNA methylation at repetitive segments of the genome, including telomeres, and undergo rapid telomere shortening and senescence (Sagie et al., 2017). As telomeric damage associated with senescence can induce broad changes to chromatin and histone biosynthesis (O'Sullivan et al., 2010), and our data suggest that the reverse may also be true; global dysfunction of the epigenome, which may be a hallmark of human aging (Zhang et al., 2015), could elicit rapid telomere instability and irreversible damage in cells that are deficient for telomerase. We propose that small RNAs could be generally relevant to lncRNA-mediated heterochromatin formation at telomeres and possibly elsewhere in the genome, such as loci that are subjected to parent-of-origin genomic imprinting (Holoach and Moazed, 2015, Taylor et al., 2015).

Finally, we note that the *C. elegans* secondary siRNA biogenesis factor MUT-7 (Figure 1A, B) is homologous to the exonuclease domain of human WRN1, which is commonly mutated in Werner's syndrome and results in early-onset aging of multiple tissues. WRN1 deficiency is accompanied by accelerated telomere erosion and senescence phenotypes that can be rescued by telomerase expression (Shimamoto et al., 2015). While WRN1 and its homologs have been intensively studied for their roles in DNA recombination, WRN1 was recently shown to safeguard the epigenomic stability of heterochromatin (Zhang et al., 2015). Our study suggests that Werner syndrome may be explained, in part, by defects in siRNA-mediated heterochromatin silencing at telomeres and elsewhere in the genome.

Materials and Methods

Strains: Unless otherwise noted, all strains were maintained at 20°C on nematode growth medium plates seeded with *Escherichia coli* OP50. Strains used include Bristol N2 ancestral, *wago-1(tm1414)*, *trt-1(ok410)*, *unc-29(e193)*, *dpy-5(e61)*, *dcr-1(mg375)*, *hrde-1(tm1200)*, *rde-1(ne219)*, *rde-4(ne299)*, *rrf-3(mg373)*, *rrf-2(ok210)*, *eri-1(mg366)*, *mut-7(pk204)*, *mut-7(pk720)*, *mut-14(pk738)*, *rbr-2(tm1231)*, *spr-5(by101)*, *xnp-1(ok1823)*, *xnp-1(tm678)*, *hpl-1(tm1624)*, *hpl-2(ok916)*, *hpl-2(tm1479)*, *exo-1(tm1842)*. A *trt-1 unc-29* double mutant, where *unc-29* is tightly linked to *trt-1*, was used to create strains used in this study. Double, triple and quadruple mutants were created using standard marker mutations and verified based on phenotype or genotype.

DAPI staining: One-day-old adults were washed twice in M9, soaked in 150 µL of 400ng/mL DAPI in ethanol solution for 30 min or until evaporated, rehydrated in 2 mL of M9 solution overnight at 4°C, and mounted in 8 µL VECTASHIELD mounting medium (Vector Laboratories). Chromosome counts were performed under 60x magnification and a 359nm excitation wavelength using a Nikon Eclipse E800 microscope.

qPCR: Non-starved mixed-stage worms were washed with M9 and RNA was extracted using 1 mL TRIZOL according to the manufacturer's instructions. For RT-PCR analysis, total RNA was treated twice with DNase I and was reverse transcribed with act-1 and a telomere-specific primer ((GCCTAA)₃) using SuperScript II reverse transcriptase (Invitrogen). For SYBR green reactions, subtelomere specific primers were designed within 200bp of the telomere-subtelomere junction.

RNA FISH: RNA FISH was performed as previously described (Sakaguchi et al., 2014) with several modifications. In brief, non-starved, mixed-stage animals were washed twice in M9 and three times in 1x DEPC-treated PBS. Worms were fixed in 1mL fixation buffer (1x DEPC-treated PBS with 3.7% formaldehyde) for 45 min rotating at room temperature then washed twice in 1mL 1x DEPC-treated PBS. Fixed animals were permeabilized overnight at 4°C in 70% ethanol in DEPC-treated H₂O, then washed in 1 mL wash buffer [10% (vol/vol) formamide in 2x RNases-free SSC]. Aliquots of each

sample were removed prior to hybridization and treated with RNaseA for 1h at 37°C to ensure probe specificity to RNA. Hybridization was performed at 30°C overnight in 100 µL hybridization buffer (10% dextran sulfate, 2x RNase-free SSC, 10% deionized formamide, 50, 0.02% RNase-free BSA, 50 µg *E. coli* tRNA) with 1.25 µM probe. Cy5-labelled (GCCTAA)₃ probe was used to detect TERRA transcripts. Animals were washed twice with wash buffer, counterstained with 25 ng/mL DAPI for 30 min at room temperature, and mounted on glass slides in VECTASHIELD mounting medium (Vector Laboratories) before epifluorescence microscopy.

IF: IF was carried out as previously described (Phillips et al., 2009) by fixing dissected gonads of 1 day old adults in 2% PFA for 10 minutes followed by a 1 minute postfixation in methanol. Rabbit anti-pS/TQ (Cell Signaling Technology) was used at a 1:500 dilution and mouse anti-RNA:DNA hybrid S9.6 at 1:500 dilution. Stained gonads were counterstained with DAPI and mounted with VECTASHIELD (Vector laboratories) before epifluorescence microscopy.

RNAi: RNAi clone expressing dsRNA targeting *C. elegans* telomeres was constructed using NEB HiFi DNA assembly mix according to the manufacturer's instructions. 200 bp of telomeric repeats were amplified from cTel55x by PCR with 20 bp overlap to Spel digested L4440. Correct constructs were transformed into HT115 and RNAi was performed as previously described (McMurchy et al., 2017).

Southern Blot: *C. elegans* genomic DNA was digested overnight with Hinf1 (New England Biolabs), separated on a 0.8% agarose gel at 1.5 V/cm, and transferred to a neutral nylon membrane (Hybond-N, GE Healthcare Life Sciences). A digoxigenin-labelled telomere probe was hybridized and detected as described (Ahmed and Hodgkin, 2000).

Mrt and ALT assays: When telomerase-deficient *trt-1(ok410)* *C. elegans* mutants are passaged by using the standard Mortal Germline (Mrt) assay developed in our laboratory, which involves passaging six L1 larval animals to fresh plates weekly, 100%

become sterile within 20–30 generations. When *trt-1(ok410)* strains are passaged weekly by transferring a 1cm² chunk of agar populated with ≈200–400 animals, 10-20% of the strains survive for hundreds of generations. Mantel-Cox Log Rank Analysis was used to determine differences of transgenerational lifespan between strains. A z-test was performed to compare proportion of ALT survivors in chunked strains.

RNA-seq: Animals were grown at 20°C on 100 mm NGM plates seeded with OP50 bacteria. Two biological replicates were prepared for each genotype. RNA was extracted using Trizol (Ambion) followed by isopropanol precipitation. RNA samples were treated with 20U RNA 5' polyphosphatase (Lucigen, RP8092H) for 30 minutes at 37°C to remove 5' triphosphate groups. Library preparation and sequencing was performed at the UNC School of Medicine High-Throughput Sequencing Facility (HTSF). RNA-seq libraries were prepared using the NEXTflex Small RNA Library Prep Kit for Illumina (Bio Scientific). Libraries were sequenced on an Illumina HiSeq 2500 to produce approximately twenty million 50 bp single-end reads per library.

Analysis of high throughput sequencing data: Publicly available RNA-seq datasets were download from the Gene Expression Omnibus (<https://www.ncbi.nlm.nih.gov/geo/>) (see table X for library information). Adapter trimming was performed as required using the bbdut.sh script from the bmap suite3 and custom scripts (Bushnell, 2016). Reads were then filtered for 22G species or all species between 18 and 30 nucleotides in length using a custom python script. Reads were then converted to fasta format and mapped to the *C. elegans* genome (WS251) using bowtie (Langmead et al., 2009) with the following options: -M 1 -v 0 -best -strata. Uniquely mapping siRNAs were detected by replacing the -M 1 parameter with -m 1. To detect telomere-mapping siRNAs, reads were mapped to seven repeats of perfect telomere sequence (TTAGGC), allowing for zero mismatches. Unmapped reads were re-mapped to the telomere sequence, this time allowing for one mismatch. This step was repeated to detect reads that map to telomeres with two or three mismatches. Genes with differential siRNA abundance in *trt-1* were identified using DESeq2 (Love et al., 2014). To detect changes in the abundance of subtelomeric siRNAs in *trt-1* and *trt-1; dcr-1*, 22G reads mapping to the

2kb of sequence adjacent to the telomere were counted for each chromosome arm. Counts were normalized by dividing by the total number of mapped reads for each library. A pseudocount of 1 was added to each normalized value to avoid division by zero errors. Replicates were averaged and the log2-fold change between mutant and wild-type was calculated for each subtelomere. Analysis of sequencing data was performed using the R statistical computing environment (Team, 2017). Genome regions were visualized using the Gviz R package (Hahne and Ivanek, 2016). Immunoprecipitation datasets were used in Figure 3G, H but were excluded from the analysis shown in Figure 3D-F. To detect siRNAs targeting transposons, 22G reads were mapped to the *C. elegans* transposon consensus sequences downloaded from Repbase with bowtie, allowing for up to two mismatches. ChIP-seq reads were mapped to the genome as fastq files as described above without the size filtering step. Read coverage was calculated at each base using bedtools (Quinlan and Hall, 2010). Coverage values were normalized by dividing by the number of total mapped reads for each library and enrichment was calculated by dividing the normalized coverage for I.P. libraries by the normalized coverage of their respective input libraries.

Accession numbers: RNA-seq data reported in this study are available under the accession number GEO: GSE111800.

Acknowledgements

We thank R. Downen for technical advice with qRT-PCR, K. Billmyre for advice on immunofluorescence, and members of the S.A. laboratory for critical review of the manuscript. Some strains were provided by the Caenorhabditis Genetics Center, which is funded by National Institutes of Health Office of Research Infrastructure Programs (P40 OD010440). S.F., C.L. and S.A. were supported by National Institute of Health grant R01 GM066228.

Competing Interests

The authors declare no competing interests.

References

- AHMED, S. & HODGKIN, J. 2000. MRT-2 checkpoint protein is required for germline immortality and telomere replication in *C. elegans*. *Nature*, 403, 159-64.
- AKAY, A., DI DOMENICO, T., SUEN, K. M., NABIH, A., PARADA, G. E., LARANCE, M., MEDHI, R., BERKYUREK, A. C., ZHANG, X., WEDELES, C. J., RUDOLPH, K. L. M., ENGELHARDT, J., HEMBERG, M., MA, P., LAMOND, A. I., CLAYCOMB, J. M. & MISKA, E. A. 2017. The Helicase Aquarius/EMB-4 Is Required to Overcome Intronic Barriers to Allow Nuclear RNAi Pathways to Heritably Silence Transcription. *Dev Cell*, 42, 241-255 e6.
- ARNOULT, N., VAN BENEDEN, A. & DECOTTIGNIES, A. 2012. Telomere length regulates TERRA levels through increased trimethylation of telomeric H3K9 and HP1alpha. *Nat Struct Mol Biol*, 19, 948-56.
- ASHE, A., SAPETSCHNIG, A., WEICK, E. M., MITCHELL, J., BAGIJN, M. P., CORDING, A. C., DOEBLEY, A. L., GOLDSTEIN, L. D., LEHRBACH, N. J., LE PEN, J., PINTACUDA, G., SAKAGUCHI, A., SARKIES, P., AHMED, S. & MISKA, E. A. 2012. piRNAs Can Trigger a Multigenerational Epigenetic Memory in the Germline of *C. elegans*. *Cell*, 150, 88-99.
- AVGOUSTI, D. C., PALANI, S., SHERMAN, Y. & GRISHOK, A. 2012. CSR-1 RNAi pathway positively regulates histone expression in *C. elegans*. *EMBO J*, 31, 3821-32.
- AZZALIN, C. M. & LINGNER, J. 2015. Telomere functions grounding on TERRA firma. *Trends Cell Biol*, 25, 29-36.
- AZZALIN, C. M., REICHENBACH, P., KHORIAULI, L., GIULOTTO, E. & LINGNER, J. 2007. Telomeric repeat containing RNA and RNA surveillance factors at mammalian chromosome ends. *Science*, 318, 798-801.
- BAGIJN, M. P., GOLDSTEIN, L. D., SAPETSCHNIG, A., WEICK, E. M., BOUASKER, S., LEHRBACH, N. J., SIMARD, M. J. & MISKA, E. A. 2012. Function, targets, and evolution of *Caenorhabditis elegans* piRNAs. *Science*, 337, 574-8.
- BATISTA, P. J., RUBY, J. G., CLAYCOMB, J. M., CHIANG, R., FAHLGREN, N., KASSCHAU, K. D., CHAVES, D. A., GU, W., VASALE, J. J., DUAN, S., CONTE, D., JR., LUO, S., SCHROTH, G. P., CARRINGTON, J. C., BARTEL, D. P. & MELLO, C. C. 2008. PRG-1 and 21U-RNAs interact to form the piRNA complex required for fertility in *C. elegans*. *Mol Cell*, 31, 67-78.
- BENETTI, R., GARCIA-CAO, M. & BLASCO, M. A. 2007. Telomere length regulates the epigenetic status of mammalian telomeres and subtelomeres. *Nat Genet*, 39, 243-50.
- BENETTI, R., SCHOEFTNER, S., MUNOZ, P. & BLASCO, M. A. 2008. Role of TRF2 in the assembly of telomeric chromatin. *Cell Cycle*, 7, 3461-8.
- BERNSTEIN, E., CAUDY, A. A., HAMMOND, S. M. & HANNON, G. J. 2001. Role for a bidentate ribonuclease in the initiation step of RNA interference. *Nature*, 409, 363-6.
- BILLI, A. C., FISCHER, S. E. & KIM, J. K. 2014. Endogenous RNAi pathways in *C. elegans*. *WormBook*, 1-49.
- BUCKLEY, B. A., BURKHART, K. B., GU, S. G., SPRACKLIN, G., KERSHNER, A., FRITZ, H., KIMBLE, J., FIRE, A. & KENNEDY, S. 2012. A nuclear Argonaute

- promotes multigenerational epigenetic inheritance and germline immortality. *Nature*, 489, 447-51.
- BUSHNELL, B. 2016. BMap short-read aligner, and other bioinformatics tools. <http://sourceforge.net/projects/bbmap/>.
- CANZIO, D., LARSON, A. & NARLIKAR, G. J. 2014. Mechanisms of functional promiscuity by HP1 proteins. *Trends Cell Biol*, 24, 377-86.
- CAO, F., LI, X., HIEW, S., BRADY, H., LIU, Y. & DOU, Y. 2009. Dicer independent small RNAs associate with telomeric heterochromatin. *RNA*, 15, 1274-81.
- CHAVEZ, J., MURILLO-MALDONADO, J. M., BAHENA, V., CRUZ, A. K., CASTANEDA-SORTIBRAN, A., RODRIGUEZ-ARNAIZ, R., ZURITA, M. & VALADEZ-GRAHAM, V. 2017. dAdd1 and dXNP prevent genome instability by maintaining HP1a localization at Drosophila telomeres. *Chromosoma*, 126, 697-712.
- CHENG, C., SHTESSEL, L., BRADY, M. M. & AHMED, S. 2012. Caenorhabditis elegans POT-2 telomere protein represses a mode of alternative lengthening of telomeres with normal telomere lengths. *Proc Natl Acad Sci U S A*, 109, 7805-10.
- CUSANELLI, E., ROMERO, C. A. & CHARTRAND, P. 2013. Telomeric noncoding RNA TERRA is induced by telomere shortening to nucleate telomerase molecules at short telomeres. *Mol Cell*, 51, 780-91.
- DAS, P. P., BAGIJN, M. P., GOLDSTEIN, L. D., WOOLFORD, J. R., LEHRBACH, N. J., SAPETSCHNIG, A., BUHECHA, H. R., GILCHRIST, M. J., HOWE, K. L., STARK, R., MATTHEWS, N., BEREZIKOV, E., KETTING, R. F., TAVARE, S. & MISKA, E. A. 2008. Piwi and piRNAs act upstream of an endogenous siRNA pathway to suppress Tc3 transposon mobility in the Caenorhabditis elegans germline. *Mol Cell*, 31, 79-90.
- DONATE, L. E. & BLASCO, M. A. 2011. Telomeres in cancer and ageing. *Philos Trans R Soc Lond B Biol Sci*, 366, 76-84.
- FLYNN, R. L., COX, K. E., JEITANY, M., WAKIMOTO, H., BRYLL, A. R., GANEM, N. J., BERSANI, F., PINEDA, J. R., SUVA, M. L., BENES, C. H., HABER, D. A., BOUSSIN, F. D. & ZOU, L. 2015. Alternative lengthening of telomeres renders cancer cells hypersensitive to ATR inhibitors. *Science*, 347, 273-7.
- FULCHER, N., DERBOVEN, E., VALUCHOVA, S. & RIHA, K. 2014. If the cap fits, wear it: an overview of telomeric structures over evolution. *Cell Mol Life Sci*, 71, 847-65.
- GENT, J. I., LAMM, A. T., PAVELEC, D. M., MANIAR, J. M., PARAMESWARAN, P., TAO, L., KENNEDY, S. & FIRE, A. Z. 2010. Distinct phases of siRNA synthesis in an endogenous RNAi pathway in C. elegans soma. *Mol Cell*, 37, 679-89.
- GOU, L. T., DAI, P., YANG, J. H., XUE, Y., HU, Y. P., ZHOU, Y., KANG, J. Y., WANG, X., LI, H., HUA, M. M., ZHAO, S., HU, S. D., WU, L. G., SHI, H. J., LI, Y., FU, X. D., QU, L. H., WANG, E. D. & LIU, M. F. 2014. Pachytene piRNAs instruct massive mRNA elimination during late spermiogenesis. *Cell Res*, 24, 680-700.
- GRAF, M., BONETTI, D., LOCKHART, A., SERHAL, K., KELLNER, V., MAICHER, A., JOLIVET, P., TEIXEIRA, M. T. & LUKE, B. 2017. Telomere Length Determines TERRA and R-Loop Regulation through the Cell Cycle. *Cell*, 170, 72-85 e14.
- GREER, E. L., MAURES, T. J., HAUSWIRTH, A. G., GREEN, E. M., LEEMAN, D. S., MARO, G. S., HAN, S., BANKO, M. R., GOZANI, O. & BRUNET, A. 2010.

- Members of the H3K4 trimethylation complex regulate lifespan in a germline-dependent manner in *C. elegans*. *Nature*, 466, 383-7.
- GU, W., SHIRAYAMA, M., CONTE, D., JR., VASALE, J., BATISTA, P. J., CLAYCOMB, J. M., MORESCO, J. J., YOUNGMAN, E. M., KEYS, J., STOLTZ, M. J., CHEN, C. C., CHAVES, D. A., DUAN, S., KASSCHAU, K. D., FAHLGREN, N., YATES, J. R., 3RD, MITANI, S., CARRINGTON, J. C. & MELLO, C. C. 2009. Distinct argonaute-mediated 22G-RNA pathways direct genome surveillance in the *C. elegans* germline. *Mol Cell*, 36, 231-44.
- HAHNE, F. & IVANEK, R. 2016. Visualizing Genomic Data Using Gviz and Bioconductor. *Methods Mol Biol*, 1418, 335-51.
- HAN, T., MANOHARAN, A. P., HARKINS, T. T., BOUFFARD, P., FITZPATRICK, C., CHU, D. S., THIERRY-MIEG, D., THIERRY-MIEG, J. & KIM, J. K. 2009. 26G endo-siRNAs regulate spermatogenic and zygotic gene expression in *Caenorhabditis elegans*. *Proc Natl Acad Sci U S A*, 106, 18674-9.
- HEARD, E. & TURNER, J. 2011. Function of the sex chromosomes in mammalian fertility. *Cold Spring Harb Perspect Biol*, 3, a002675.
- HOLOCH, D. & MOAZED, D. 2015. RNA-mediated epigenetic regulation of gene expression. *Nat Rev Genet*, 16, 71-84.
- HOLOHAN, B., WRIGHT, W. E. & SHAY, J. W. 2014. Cell biology of disease: Telomeropathies: an emerging spectrum disorder. *J Cell Biol*, 205, 289-99.
- KETTING, R. F., FISCHER, S. E., BERNSTEIN, E., SIJEN, T., HANNON, G. J. & PLASTERK, R. H. 2001. Dicer functions in RNA interference and in synthesis of small RNA involved in developmental timing in *C. elegans*. *Genes Dev*, 15, 2654-9.
- KETTING, R. F., HAVERKAMP, T. H., VAN LUENEN, H. G. & PLASTERK, R. H. 1999. Mut-7 of *C. elegans*, required for transposon silencing and RNA interference, is a homolog of Werner syndrome helicase and RNaseD. *Cell*, 99, 133-41.
- KNIGHT, S. W. & BASS, B. L. 2001. A role for the RNase III enzyme DCR-1 in RNA interference and germ line development in *Caenorhabditis elegans*. *Science*, 293, 2269-71.
- LANGMEAD, B., TRAPNELL, C., POP, M. & SALZBERG, S. L. 2009. Ultrafast and memory-efficient alignment of short DNA sequences to the human genome. *Genome Biol*, 10, R25.
- LI, F., HUARTE, M., ZARATIEGUI, M., VAUGHN, M. W., SHI, Y., MARTIENSSEN, R. & CANDE, W. Z. 2008. Lid2 is required for coordinating H3K4 and H3K9 methylation of heterochromatin and euchromatin. *Cell*, 135, 272-83.
- LI, J. S., MIRALLES FUSTE, J., SIMAVORIAN, T., BARTOCCI, C., TSAI, J., KARLSEDER, J. & LAZZERINI DENCHI, E. 2017. TZAP: A telomere-associated protein involved in telomere length control. *Science*, 355, 638-641.
- LOVE, M. I., HUBER, W. & ANDERS, S. 2014. Moderated estimation of fold change and dispersion for RNA-seq data with DESeq2. *Genome Biol*, 15, 550.
- LOVEJOY, C. A., LI, W., REISENWEBER, S., THONGTHIP, S., BRUNO, J., DE LANGE, T., DE, S., PETRINI, J. H., SUNG, P. A., JASIN, M., ROSENBLUH, J., ZWANG, Y., WEIR, B. A., HATTON, C., IVANOVA, E., MACCONAILL, L., HANNA, M., HAHN, W. C., LUE, N. F., REDDEL, R. R., JIAO, Y., KINZLER, K., VOGELSTEIN, B., PAPADOPOULOS, N., MEEKER, A. K. & CONSORTIUM, A.

- 796 L. T. S. C. 2012. Loss of ATRX, genome instability, and an altered DNA damage
797 response are hallmarks of the alternative lengthening of telomeres pathway.
798 *PLoS Genet*, 8, e1002772.
- 799 MACIEJOWSKI, J. & DE LANGE, T. 2017. Telomeres in cancer: tumour suppression
800 and genome instability. *Nat Rev Mol Cell Biol*, 18, 175-186.
- 801 MAICHER, A., KASTNER, L., DEES, M. & LUKE, B. 2012. Deregulated telomere
802 transcription causes replication-dependent telomere shortening and promotes
803 cellular senescence. *Nucleic Acids Res*, 40, 6649-59.
- 804 MCMURCHY, A. N., STEMPOR, P., GAARENSTROOM, T., WYSOLMERSKI, B.,
805 DONG, Y., AUSSIANIKAVA, D., APPERT, A., HUANG, N., KOLASINSKA-
806 ZWIERZ, P., SAPETSCHNIG, A., MISKA, E. A. & AHRINGER, J. 2017. A team
807 of heterochromatin factors collaborates with small RNA pathways to combat
808 repetitive elements and germline stress. *Elife*, 6.
- 809 MORAVEC, M., WISCHNEWSKI, H., BAH, A., HU, Y., LIU, N., LAFRANCHI, L., KING,
810 M. C. & AZZALIN, C. M. 2016. TERRA promotes telomerase-mediated telomere
811 elongation in *Schizosaccharomyces pombe*. *EMBO Rep*, 17, 999-1012.
- 812 O'SULLIVAN, R. J., KUBICEK, S., SCHREIBER, S. L. & KARLSEDER, J. 2010.
813 Reduced histone biosynthesis and chromatin changes arising from a damage
814 signal at telomeres. *Nat Struct Mol Biol*, 17, 1218-25.
- 815 ORTIZ, M. A., NOBLE, D., SOROKIN, E. P. & KIMBLE, J. 2014. A new dataset of
816 spermatogenic vs. oogenic transcriptomes in the nematode *Caenorhabditis*
817 *elegans*. *G3 (Bethesda)*, 4, 1765-72.
- 818 PAK, J. & FIRE, A. 2007. Distinct populations of primary and secondary effectors during
819 RNAi in *C. elegans*. *Science*, 315, 241-4.
- 820 PARDUE, M. L. & DEBARYSHE, P. G. 2003. Retrotransposons provide an
821 evolutionarily robust non-telomerase mechanism to maintain telomeres. *Annu*
822 *Rev Genet*, 37, 485-511.
- 823 PFEIFFER, V. & LINGNER, J. 2012. TERRA promotes telomere shortening through
824 exonuclease 1-mediated resection of chromosome ends. *PLoS Genet*, 8,
825 e1002747.
- 826 PHILLIPS, C. M., MCDONALD, K. L. & DERNBURG, A. F. 2009. Cytological analysis of
827 meiosis in *Caenorhabditis elegans*. *Methods Mol Biol*, 558, 171-95.
- 828 PICKETT, H. A. & REDDEL, R. R. 2015. Molecular mechanisms of activity and
829 derepression of alternative lengthening of telomeres. *Nat Struct Mol Biol*, 22,
830 875-80.
- 831 PORRO, A., FEUERHAHN, S., DELAFONTAINE, J., RIETHMAN, H., ROUGEMONT, J.
832 & LINGNER, J. 2014. Functional characterization of the TERRA transcriptome at
833 damaged telomeres. *Nat Commun*, 5, 5379.
- 834 QUINLAN, A. R. & HALL, I. M. 2010. BEDTools: a flexible suite of utilities for comparing
835 genomic features. *Bioinformatics*, 26, 841-2.
- 836 REINHART, B. J. & BARTEL, D. P. 2002. Small RNAs correspond to centromere
837 heterochromatic repeats. *Science*, 297, 1831.
- 838 ROSSIello, F., AGUADO, J., SEPE, S., IANNELLI, F., NGUYEN, Q., PITCHIAYA, S.,
839 CARNINCI, P. & D'ADDA DI FAGAGNA, F. 2017. DNA damage response
840 inhibition at dysfunctional telomeres by modulation of telomeric DNA damage
841 response RNAs. *Nat Commun*, 8, 13980.

- 842 SAGIE, S., TOUBIANA, S., HARTONO, S. R., KATZIR, H., TZUR-GILAT, A.,
843 HAVAZELET, S., FRANCASTEL, C., VELASCO, G., CHEDIN, F. & SELIG, S.
844 2017. Telomeres in ICF syndrome cells are vulnerable to DNA damage due to
845 elevated DNA:RNA hybrids. *Nat Commun*, 8, 14015.
- 846 SAKAGUCHI, A., SARKIES, P., SIMON, M., DOEBLEY, A. L., GOLDSTEIN, L. D.,
847 HEDGES, A., IKEGAMI, K., ALVARES, S. M., YANG, L., LAROCQUE, J. R.,
848 HALL, J., MISKA, E. A. & AHMED, S. 2014. Caenorhabditis elegans RSD-2 and
849 RSD-6 promote germ cell immortality by maintaining small interfering RNA
850 populations. *Proc Natl Acad Sci U S A*, 111, E4323-31.
- 851 SCHAETZLEIN, S., KODANDARAMIREDDY, N. R., JU, Z., LECHER, A.,
852 STEPCZYNSKA, A., LILLI, D. R., CLARK, A. B., RUDOLPH, C., KUHNEL, F.,
853 WEI, K., SCHLEGELBERGER, B., SCHIRMACHER, P., KUNKEL, T. A.,
854 GREENBERG, R. A., EDELMANN, W. & RUDOLPH, K. L. 2007. Exonuclease-1
855 deletion impairs DNA damage signaling and prolongs lifespan of telomere-
856 dysfunctional mice. *Cell*, 130, 863-77.
- 857 SHAY, J. W. 2016. Role of Telomeres and Telomerase in Aging and Cancer. *Cancer*
858 *Discov*, 6, 584-93.
- 859 SHIMAMOTO, A., YOKOTE, K. & TAHARA, H. 2015. Werner Syndrome-specific
860 induced pluripotent stem cells: recovery of telomere function by reprogramming.
861 *Front Genet*, 6, 10.
- 862 SHIRAYAMA, M., STANNEY, W., 3RD, GU, W., SETH, M. & MELLO, C. C. 2014. The
863 Vasa Homolog RDE-12 engages target mRNA and multiple argonaute proteins to
864 promote RNAi in C. elegans. *Curr Biol*, 24, 845-51.
- 865 STEINER, F. A., OKIHARA, K. L., HOOGSTRATE, S. W., SIJEN, T. & KETTING, R. F.
866 2009. RDE-1 slicer activity is required only for passenger-strand cleavage during
867 RNAi in Caenorhabditis elegans. *Nat Struct Mol Biol*, 16, 207-11.
- 868 TABARA, H., YIGIT, E., SIOMI, H. & MELLO, C. C. 2002. The dsRNA binding protein
869 RDE-4 interacts with RDE-1, DCR-1, and a DEXH-box helicase to direct RNAi in
870 C. elegans. *Cell*, 109, 861-71.
- 871 TAYLOR, D. H., CHU, E. T., SPEKTOR, R. & SOLOWAY, P. D. 2015. Long non-coding
872 RNA regulation of reproduction and development. *Mol Reprod Dev*, 82, 932-56.
- 873 TEAM, R. C. 2017. R: A language and environment for statistical computing. R
874 Foundation for Statistical Computing, Vienna, Austria. <https://www.R-project.org/>.
- 875 TIJSTERMAN, M., KETTING, R. F., OKIHARA, K. L., SIJEN, T. & PLASTERK, R. H.
876 2002. RNA helicase MUT-14-dependent gene silencing triggered in C. elegans
877 by short antisense RNAs. *Science*, 295, 694-7.
- 878 UDUGAMA, M., FT, M. C., CHAN, F. L., TANG, M. C., PICKETT, H. A., JD, R. M.,
879 MAYNE, L., COLLAS, P., MANN, J. R. & WONG, L. H. 2015. Histone variant
880 H3.3 provides the heterochromatic H3 lysine 9 tri-methylation mark at telomeres.
881 *Nucleic Acids Res*, 43, 10227-37.
- 882 VRBSKY, J., AKIMCHEVA, S., WATSON, J. M., TURNER, T. L., DAXINGER, L.,
883 VYSKOT, B., AUFSATZ, W. & RIHA, K. 2010. siRNA-mediated methylation of
884 Arabidopsis telomeres. *PLoS Genet*, 6, e1000986.
- 885 WEDELES, C. J., WU, M. Z. & CLAYCOMB, J. M. 2013. Protection of germline gene
886 expression by the C. elegans Argonaute CSR-1. *Dev Cell*, 27, 664-71.

- WELKER, N. C., PAVELEC, D. M., NIX, D. A., DUCHAINE, T. F., KENNEDY, S. & BASS, B. L. 2010. Dicer's helicase domain is required for accumulation of some, but not all, *C. elegans* endogenous siRNAs. *RNA*, 16, 893-903.
- WICKY, C., VILLENEUVE, A. M., LAUPER, N., CODOUREY, L., TOBLER, H. & MULLER, F. 1996. Telomeric repeats (TTAGGC)_n are sufficient for chromosome capping function in *Caenorhabditis elegans*. *Proc Natl Acad Sci U S A*, 93, 8983-8.
- WONG, L. H., MCGHIE, J. D., SIM, M., ANDERSON, M. A., AHN, S., HANNAN, R. D., GEORGE, A. J., MORGAN, K. A., MANN, J. R. & CHOO, K. H. 2010. ATRX interacts with H3.3 in maintaining telomere structural integrity in pluripotent embryonic stem cells. *Genome Res*, 20, 351-60.
- ZELLER, P., PADEKEN, J., VAN SCHENDEL, R., KALCK, V., TIJSTERMAN, M. & GASSER, S. M. 2016. Histone H3K9 methylation is dispensable for *Caenorhabditis elegans* development but suppresses RNA:DNA hybrid-associated repeat instability. *Nat Genet*, 48, 1385-1395.
- ZHANG, W., LI, J., SUZUKI, K., QU, J., WANG, P., ZHOU, J., LIU, X., REN, R., XU, X., OCAMPO, A., YUAN, T., YANG, J., LI, Y., SHI, L., GUAN, D., PAN, H., DUAN, S., DING, Z., LI, M., YI, F., BAI, R., WANG, Y., CHEN, C., YANG, F., LI, X., WANG, Z., AIZAWA, E., GOEBL, A., SOLIGALLA, R. D., REDDY, P., ESTEBAN, C. R., TANG, F., LIU, G. H. & BELMONTE, J. C. 2015. Aging stem cells. A Werner syndrome stem cell model unveils heterochromatin alterations as a driver of human aging. *Science*, 348, 1160-3.

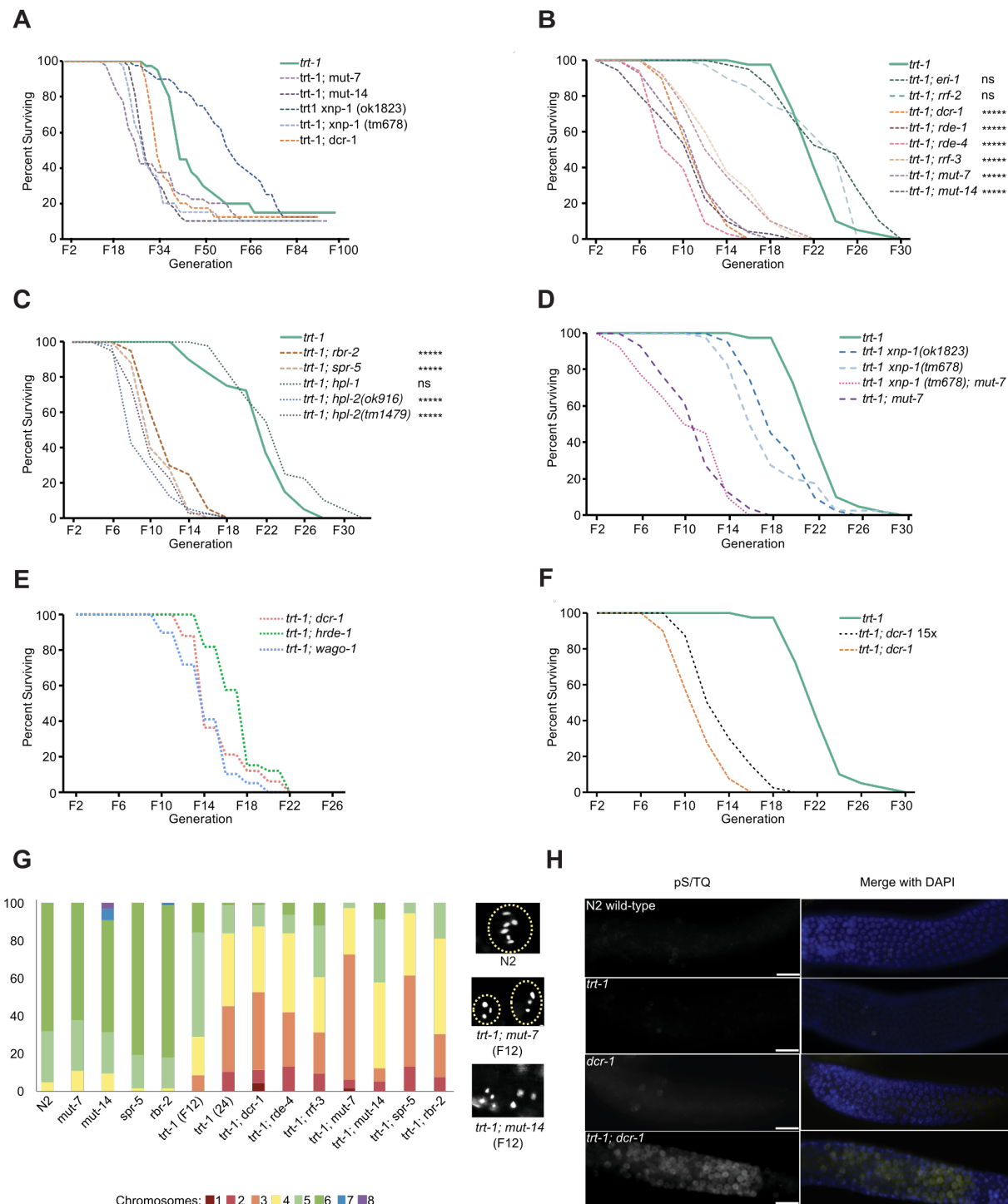


Figure 1: Endogenous small RNA and chromatin factors repress telomere stability in the absence of telomerase. (A) Survival curve of primary or secondary siRNA deficient telomerase mutants when 6 larval L1s are passaged weekly. (B) Survival curve of double mutants for *trt-1* and chromatin factors passaged by 6 L1s weekly. (C) Histone H3.3 remodeling protein XNP-1 represses senescence in *trt-1* mutants epistatically to the small RNA factor MUT-7. (D) Survival curve of telomerase-deficient strains

passaged at ~100 worms weekly for 40 independent lines. One allele of *xnp-1* (ok1823) extended survival but did not increase survival via ALT (Table S1). (E) Small RNA and heterochromatin mutant *trt-1* lines have high levels of chromosome fusions, comparable to *tr-1* single mutants at F24. Fusions were assayed by diamidino-2-phenylindole (DAPI) staining of oocytes in diakinesis. (F) High levels of phospho-(Ser/Thr) staining in the meiotic gonad of *trt-1*; *dcr-1* at F6 compared to N2 or *trt-1*. Scale bar, 25 μ m. (B)-(D) *** $p < 0.001$; **** $p < 0.00001$; ns, not significant, (Log rank test, $n \geq 40$ independent lines for each genotype).

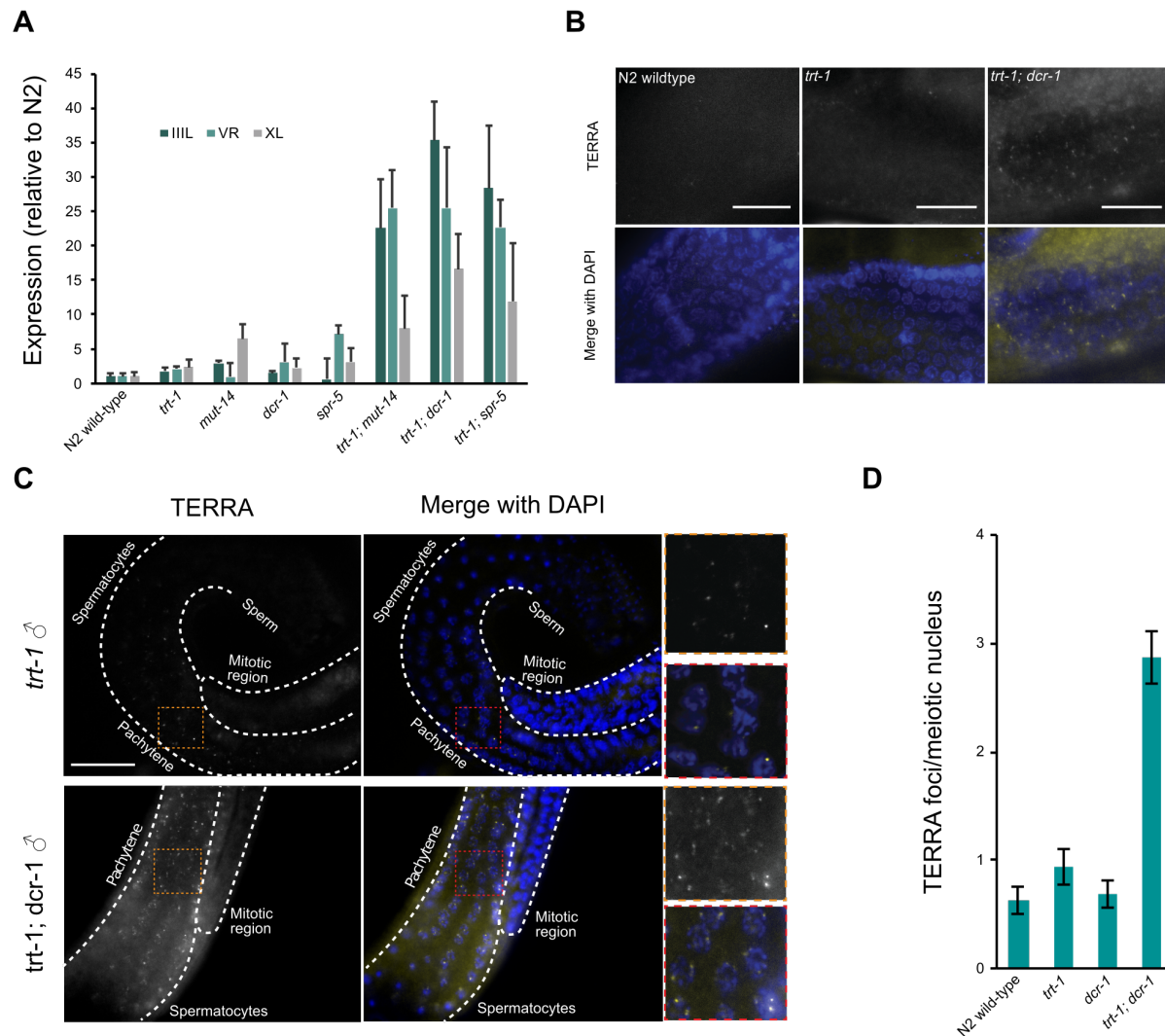


Figure 2: (A) Expression of TERRA from subtelomeres IIIIL, VR, and XL is increased in siRNA and heterochromatin deficient telomerase mutants. cDNA was reverse transcribed with a telomere specific primer and qPCR was performed using subtelomere-specific primer pairs and normalized to *act-1*. Expression data are plotted relative to wildtype and represent the mean \pm SEM of three biological replicates. (B) RNA FISH signals of TERRA in meiotic germlines of hermaphrodites of the indicated genotypes. TERRA foci are present in wildtype and *trt-1* in the pachytene region and increased in *trt-1; dcr-1*. Scale bar, 10um. (C) Representative RNA FISH images of TERRA in males show foci in the pachytene region of the germline which are increased in *trt-1; dcr-1* compared to *trt-1*. Scale bar, 20 um. (D) Quantification of germline TERRA foci (mean \pm SEM, N=10 germlines).

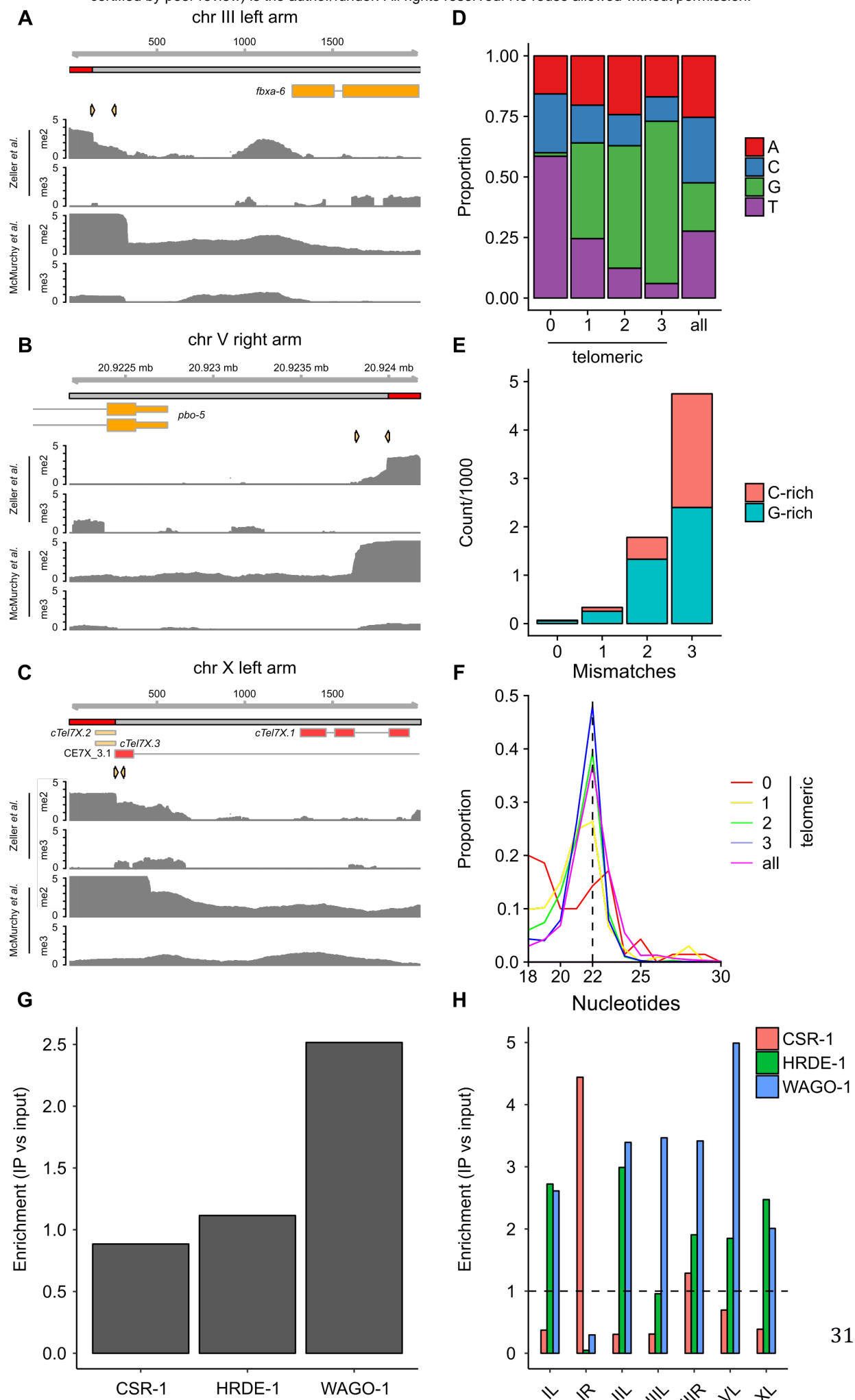


Figure 3: Analysis of telomere-mapping small RNAs in published datasets. (A)-(C) ChIP-seq enrichment profiles at three chromosome ends constructed using published data (McMurchy et al., 2017, Zeller et al., 2016). Small orange arrows between gene models and data tracks show the position of primers used in TERRA qRT-PCR experiments. (D) Proportion of telomere-mapping small RNA reads in published data beginning with a particular nucleotide. (E) Number of reads in published data mapping to the G-rich (TTAGGC) or C-rich (GCCTAA) telomeric strand. (F) Distribution of small RNA length in published data. (G) Enrichment (IP/input) of reads mapping to perfect telomere sequence with up to three mismatches in published immunoprecipitation datasets for three different Argonaute proteins. (H) Enrichment for subtelomeric siRNAs for datasets used in (G). Numbers 0-3 in (D), (E) and (F) indicate number of mismatches with perfect telomere.

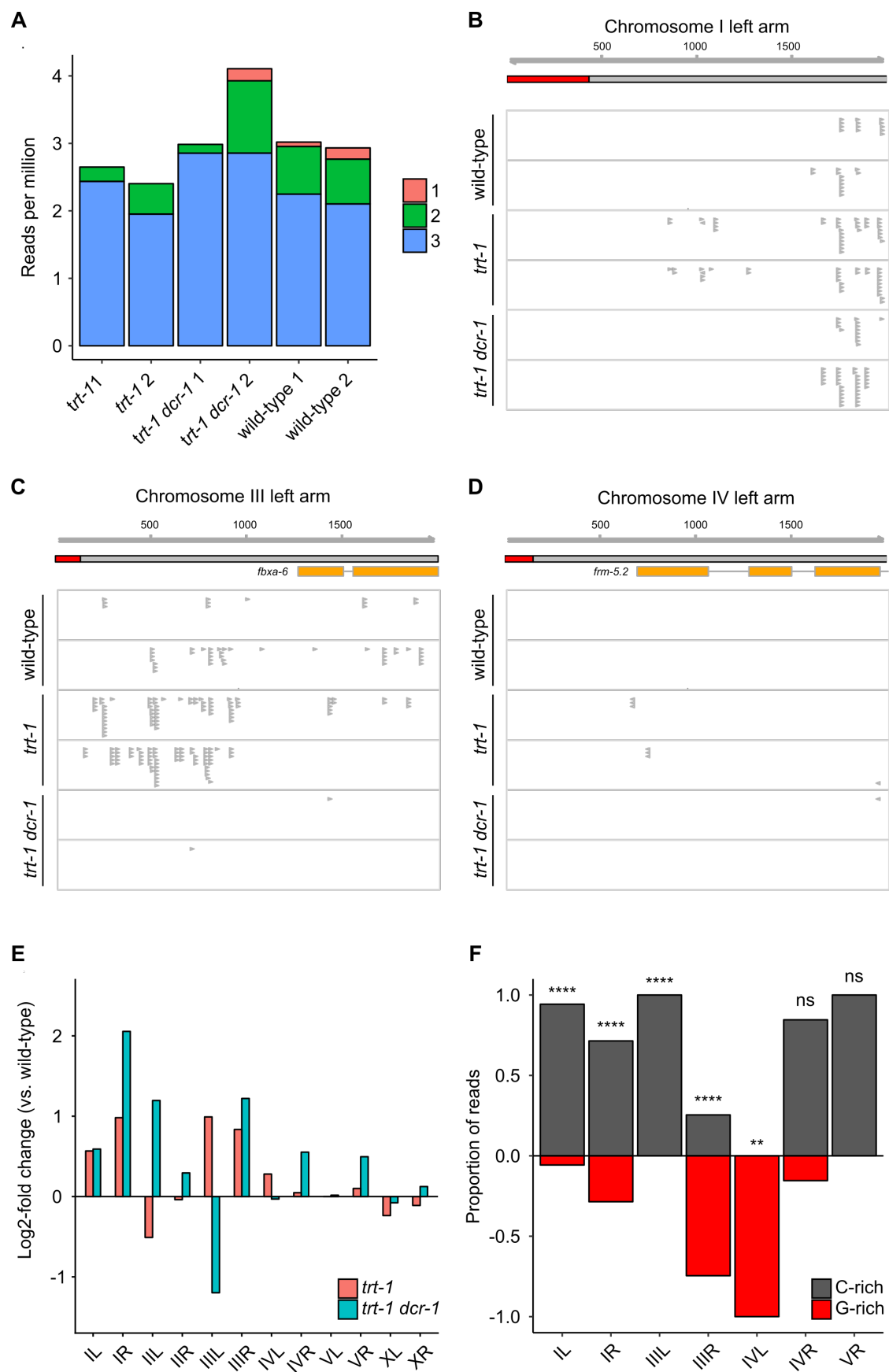


Figure 4: Upregulation of subtelomeric siRNAs in telomerase mutants. (A) Number of telomere-mapping reads in wild-type, *trt-1* and *trt-1;dcr-1* libraries. Numbers 1-3 indicate number of mismatches. (B)-(D) 22G siRNAs at three subtelomeres. (E) Log2-fold change in siRNA abundance at subtelomeres relative to wild-type in *trt-1* and *trt-1 dcr-1* animals. (F) Proportion of subtelomeric siRNAs mapping to the strand corresponding to the G-rich (TTAGGC) and C-rich (TAAGCC) telomere strand in *trt-1* animals. **** $p < 0.0001$; ** $p < 0.01$; ns, not significant (Binomial test with Bonferroni correction).

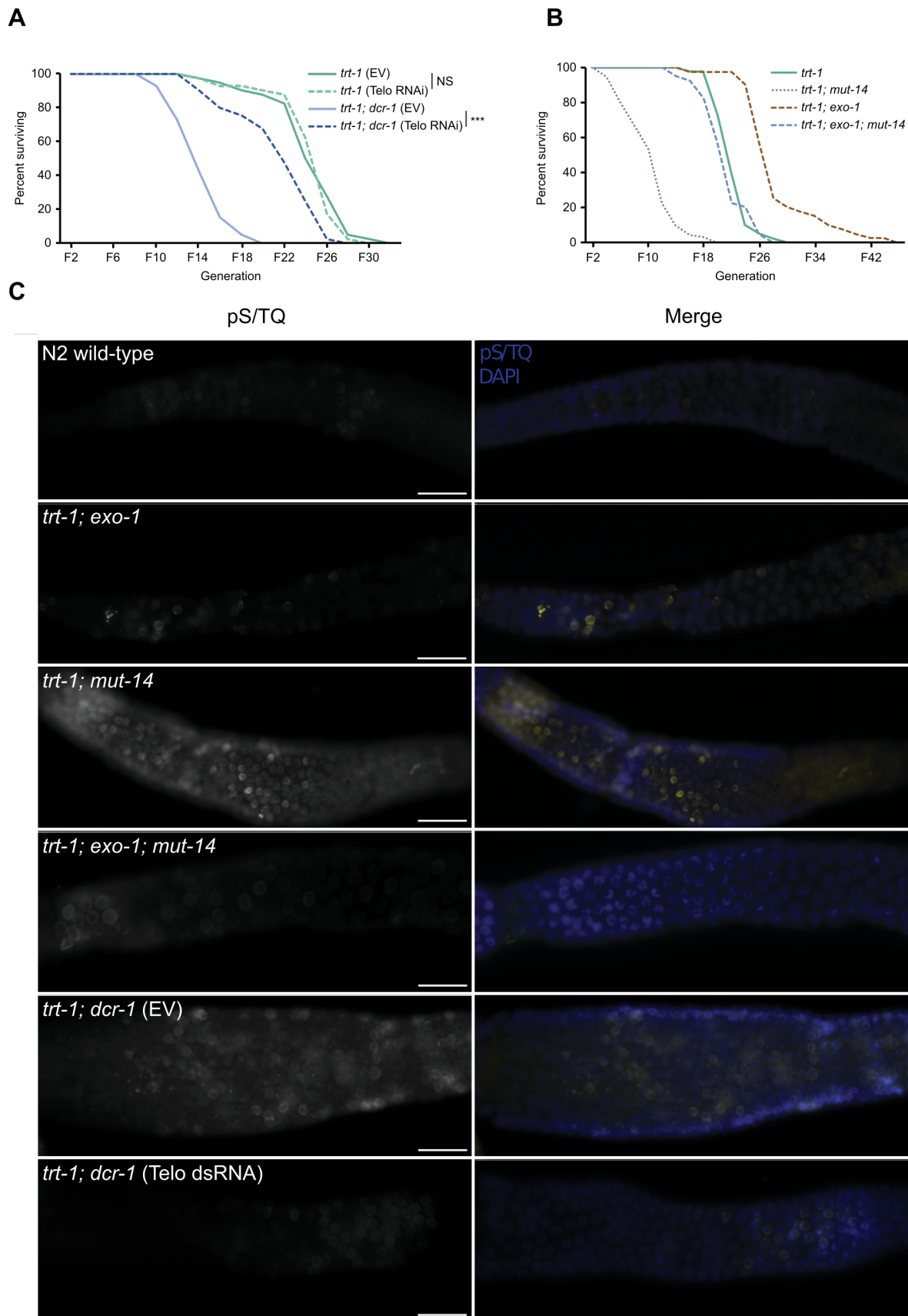


Figure 5 Fast senescence in siRNA-deficient *trt-1* is rescued by exogenous telomeric dsRNA or loss of Exonuclease-1. (A) Survival of *trt-1* or *trt-1; dcr-1(mg375)* on either empty vector control (EV) or bacteria expressing telomeric double-stranded RNA (telo dsRNA). Log rank test relative to EV, ***P < 0.001 (B) Loss of *exo-1* extends survival of *trt-1; mut-14* lines. (C) Telomeric dsRNA and loss of *exo-1* suppress accumulation of phospho-(Ser/Thr) in siRNA-deficient *trt-1* by F6. Scale bar, 20um.

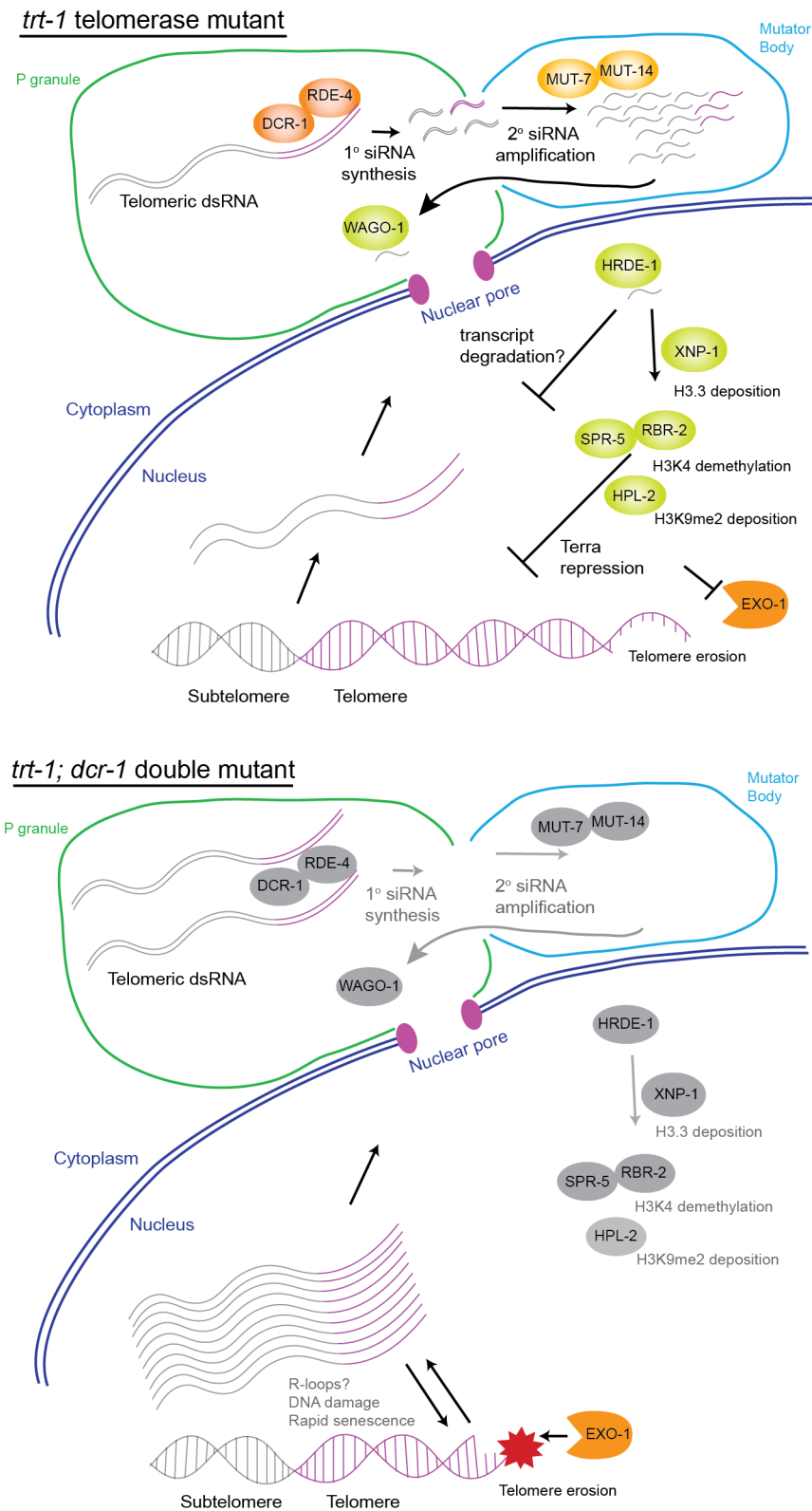


Figure 6: Model. In *trt-1* telomerase mutants, telomeric erosion induces expression of the lncRNA TERRA, which engages production of sub-telomeric and telomeric siRNAs.

Small RNAs promote deposition of H3K9me2 and H3K4 demethylation to maintain heterochromatic silencing of the telomere, repressing excess transcription, R-loop formation, DNA damage, and rapid senescence. In *trt-1; dcr-1* double mutants, TERRA expression is not repressed, leading to DNA damage, possibly RNA:DNA hybrids, and rapid senescence, which is dependent on the nuclease EXO-1.

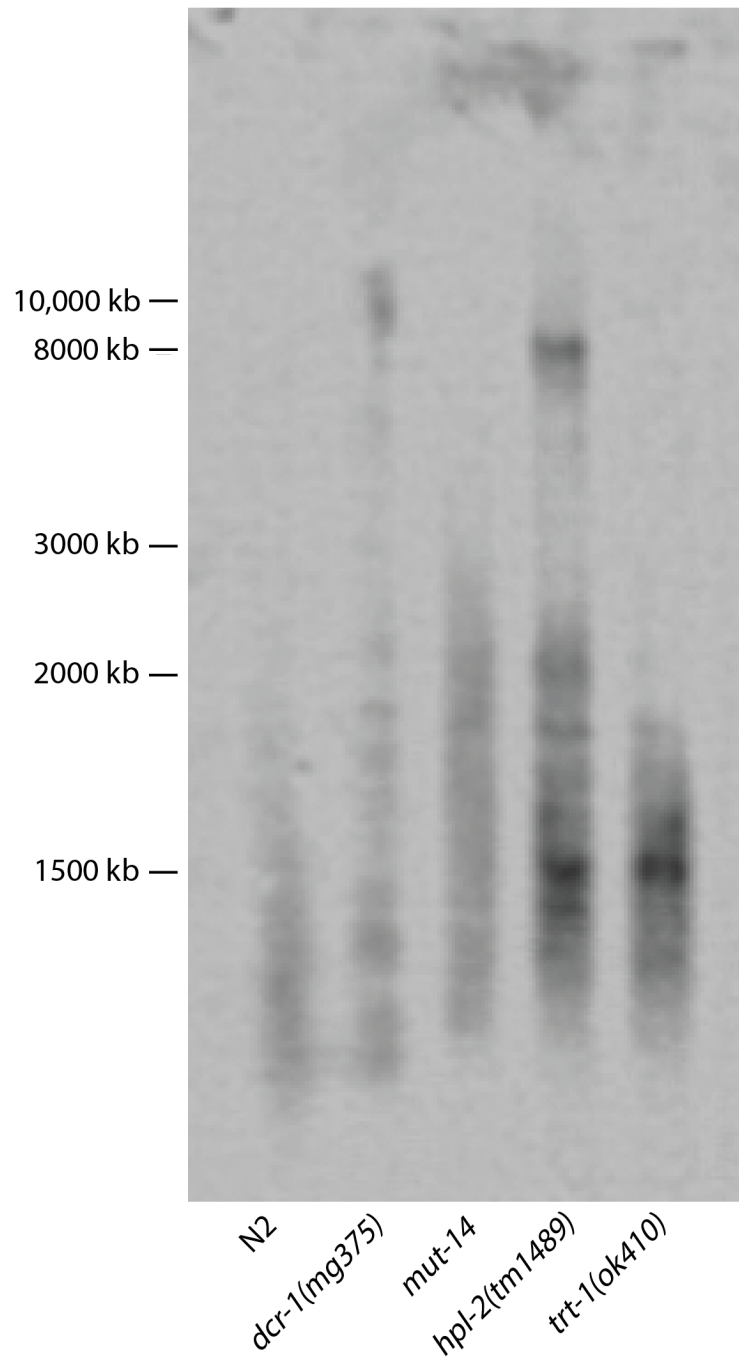
Supplemental Information

5 Supplemental Figures

3 Supplemental Tables

1 Supplemental File

S1



1007 **Figure S1. Related to Figure 1.** Terminal Restriction Fragment (TFR) analysis of
1008 wildtype and single mutant strains using a telomeric probe.

S2

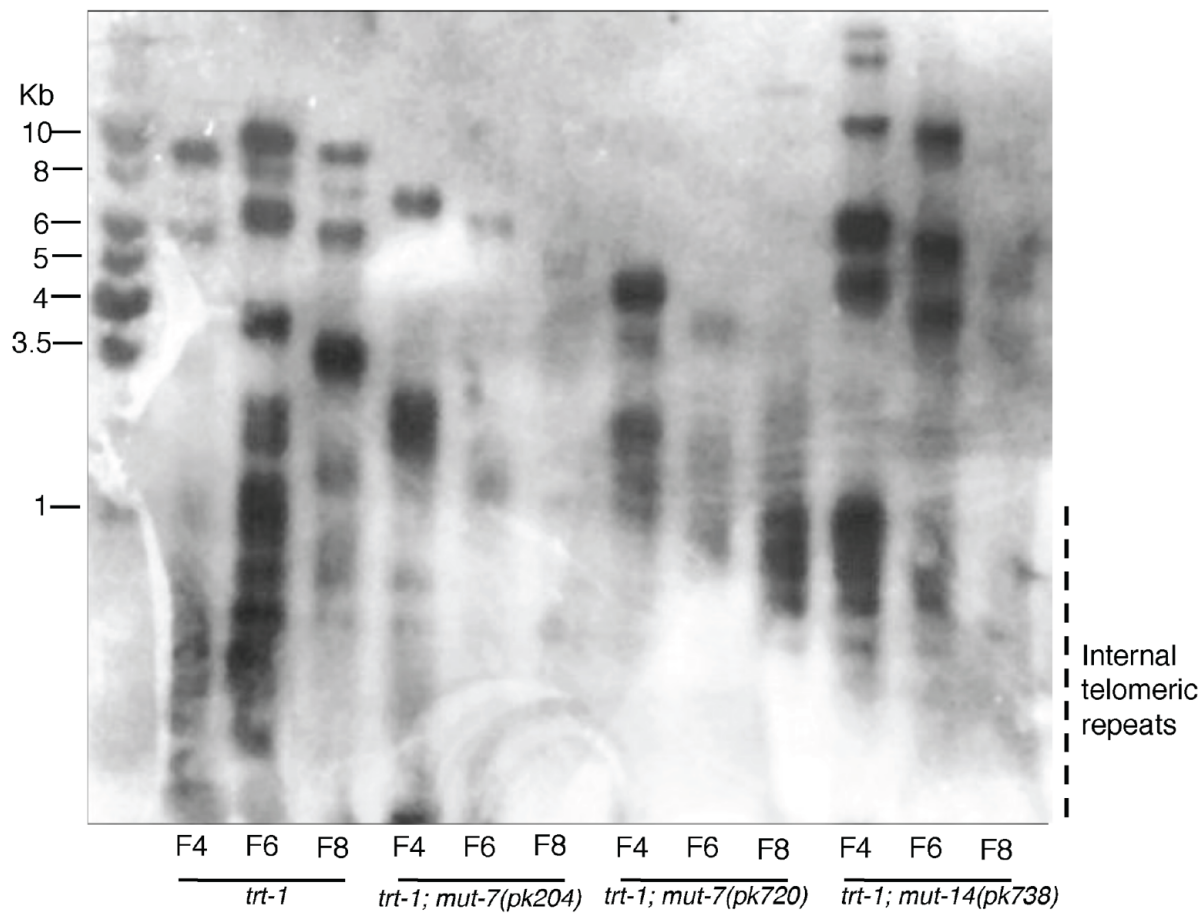


Figure S2. Related to Figure 1. TRF analysis of RNAi-deficient telomerase mutant strains using telomeric probe.

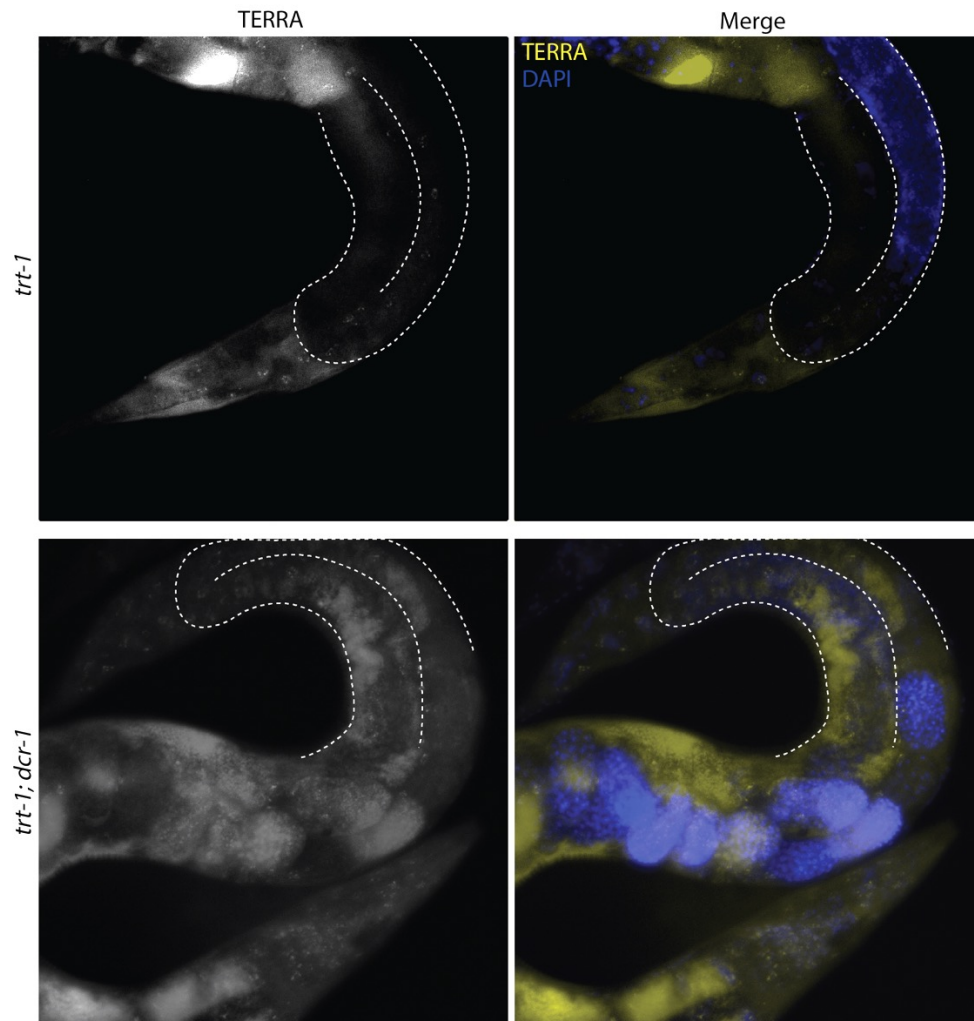


Figure S3. Related to Figure 2. TERRA expression (yellow) in *trt-1* and *trt-1; dcr-1(mg375)* 1 day old adults detected with a Cy5-labelled telomeric probe.

S4

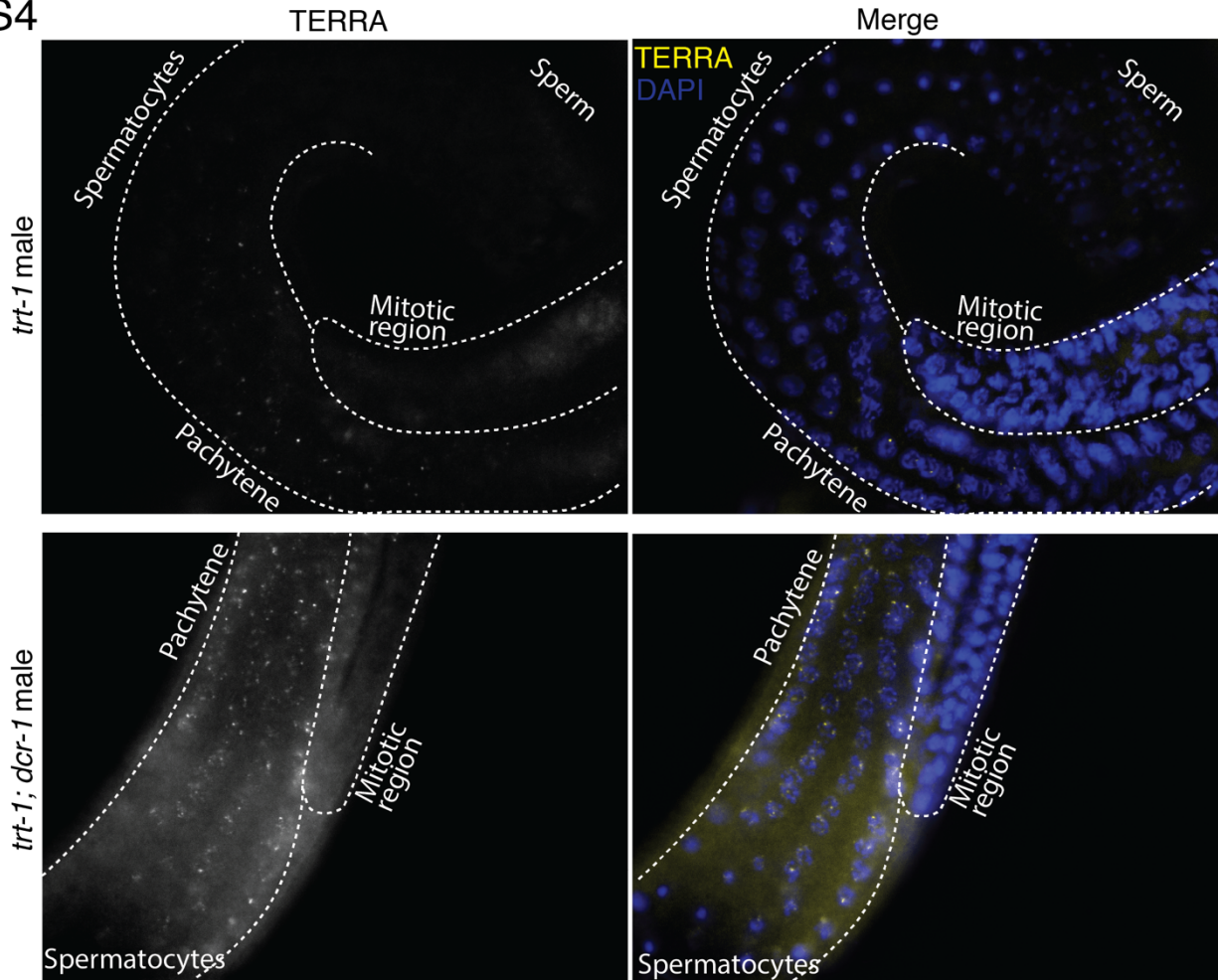


Figure S4. Related to Figure 2. RNA FISH of TERRA expression in *trt-1* and *trt-1; dcr-1* males. Note TERRA foci in the Pachytene region in both *trt-1* and *trt-1; dcr-1*, as well as lack of expression in the mitotic region and spermatocytes

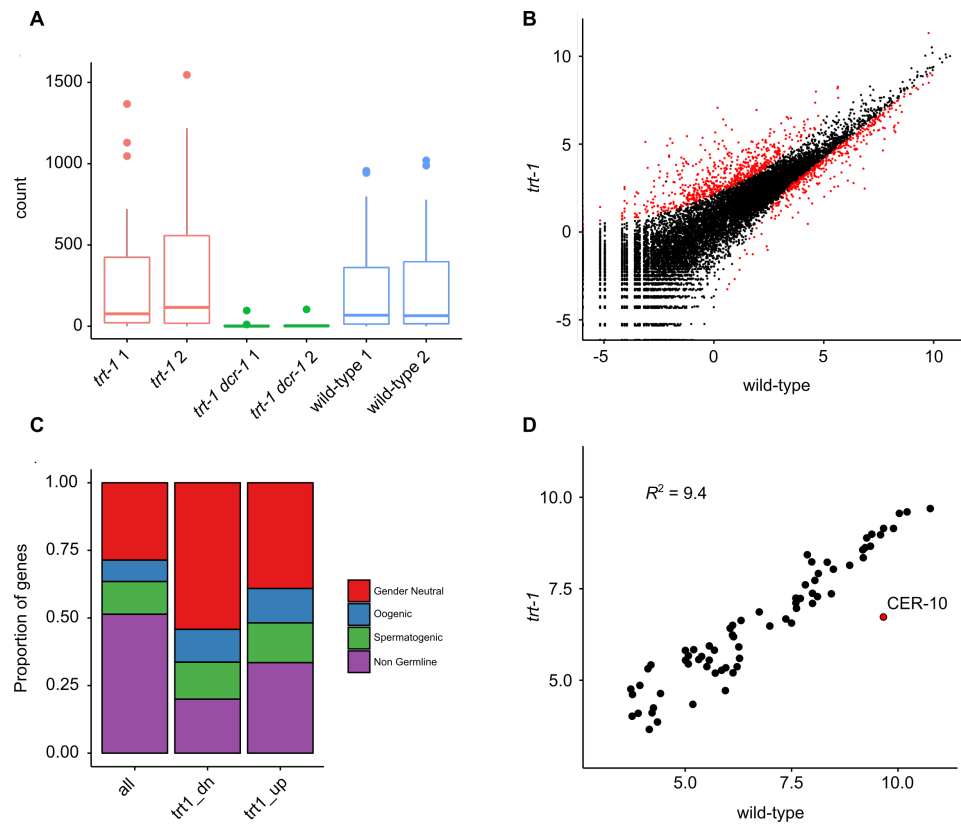


Figure S5. Related to Figure 3. Analysis of 22G small RNA species in telomerase and Dicer mutants. (A) Number of reads mapping to DCR-1 targets identified by Gent *et al.* (Gent *et al.*, 2010). (B) log2 normalized mean read counts at every *C. elegans* gene for *trt-1* and wild-type. Genes identified as significantly differentially expressed by DESeq2 are shown in red. (C) Proportion of all genes or genes downregulated (*trt1_dn*) or upregulated (*trt1_up*) belonging to expression categories defined by Ortiz *et al.* (see reference 54 in main text). (D) log2 normalized mean read counts at transposon consensus sequences for *trt-1* and wild-type.

	Lines tested	Number ALT Survivors	Z score	p-value (two tailed)
<i>trt-1</i>	40	6		
<i>trt-1; mut-7(pk204)</i>	40	4	0.6761	0.4965
<i>trt-1; mut-14(pk738)</i>	40	4	0.6761	0.4965
<i>trt-1 xnp-1(ok1823)</i>	40	6	0	1
<i>trt-1 xnp-1(tm678)</i>	40	4	0.6761	0.4965
<i>trt-1; dcr-1 (mg375)</i>	40	5	0.3247	0.7489

Supplemental Table S1. Related to Figure 1. Statistical analysis of ALT survival strains. Loss of endogenous siRNA production (*mut-7*, *mut-14*, and *dcr-1*) or histone chaperone XNP-1/ATRAX does not increase survival via ALT.

Strain	Log Rank test (Z=)	p-value
<i>trt-1; mut-7(pk204)</i>	9.79	<0.00001
<i>trt-1; mut-14(pk738)</i>	9.96	<0.00001
<i>trt-1; dcr-1(mg375)</i>	9.37	<0.00001
<i>trt-1; rde-1</i>	8.23	<0.00001
<i>trt-1; rde-4</i>	9.21	<0.00001
<i>trt-1; rrf-3</i>	8.4	<0.00001
<i>trt-1; rrf-2</i>	1.7	0.089
<i>trt-1; exo-1</i>	7.38	<0.00001
<i>trt-1 xnp-1(ok1823)</i>	4.3	<0.00001
<i>trt-1 xnp-1(tm678)</i>	4.23	<0.0001
<i>trt-1 xnp-1(tm678); mut-7</i>	9.21	<0.00001
<i>trt-1; sid-1</i>	6.52	<0.00001
<i>trt-1; rbr-2(tm1231)</i>	8.64	<0.00001
<i>trt-1; spr-5 (by101)</i>	8.89	<0.00001

Supplemental Table S2. Related to Figure 1. Log rank analysis of survival curves. N=40 independent lines for each genotype. Strains were passaged by transferring 6 larval L1s weekly and scored as sterile when plates contained no new L1 larvae.

<i>trt-1</i> F1	males	dead embryos	<i>trt-1; dcr-1</i> F1	males	dead embryos
A1	13	6	A1	0	0
A2	4	26	A2	0	0
A3	8	24	A3	1	0
D1	10	11	A4	0	0
D2	11	4	B1	0	0
D3	4	9	B2	0	0
D4	13	15	B3	0	0
			B4	0	0
			C1	0	0
			C2	0	6
			C3	1	0
			C4	0	0
			D1	0	0
			D2	0	0
			D3	0	0
			D4	0	0

Supplemental Table S3. Related to Figure 1. Counts of total F2 males and dead embryos scored for F1 progeny from crosses of wildtype males with either late-generation F16 *trt-1* mutant controls (n=2 independently grown strains, three F1 scored for strain A and four for strain D) or early generation F4 *trt-1; dcr-1* double mutant (n=4 strains, 4 F1 each scored for strains A, B, C and D) hermaphrodites. If a chromosome fusion is present in any of the F1 animals, then it will cause weak non-disjunction of the fused chromosomes, which leads to F2 dead embryos if an autosome is fused or to F2 males if the X chromosome is fused.

Supplemental File 1. Related to Figure 3. Levels of telomeric siRNAs from wild-type and those of small RNA mutants.